Atmos. Chem. Phys., 14, 5089–5110, 2014
www.atmos-chem-phys.net/14/5089/2014/
doi:10.5194/acp-14-5089-2014

Atmospheric Chemistry and Physics
Open Access

Primary and secondary biomass burning aerosols determined by proton nuclear magnetic resonance (^{1}H-NMR) spectroscopy during the 2008 EUCAARI campaign in the Po Valley (Italy)

M. Paglione[1], S. Saarikoski[2], S. Carbone[2], R. Hillamo[2], M. C. Facchini[1], E. Finessi[1], L. Giulianelli[1], C. Carbone[1], S. Fuzzi[1], F. Moretti[3], E. Tagliavini[3], E. Swietlicki[4], K. Eriksson Stenström[4], A. S. H. Prévôt[5], P. Massoli[6], M. Canaragatna[6], D. Worsnop[6], and S. Decesari[1]

[1]National Research Council (CNR), Institute of Atmospheric Sciences and Climate (ISAC), Bologna, Italy
[2]Finnish Meteorological Institute, Air Quality, Helsinki, Finland
[3]Centro Interdipartimentale di Ricerca per le Scienze Ambientali (CIRSA), University of Bologna, Ravenna, Italy
[4]Lund University, Department of Physics, Lund, Sweden
[5]Paul Scherrer Institute (PSI), Laboratory of Atmospheric Chemistry, Villigen, Switzerland
[6]Aerodyne Research, Inc. Billerica, MA, USA

Correspondence to: M. Paglione (m.paglione@isac.cnr.it)

Received: 29 November 2013 – Published in Atmos. Chem. Phys. Discuss.: 19 December 2013
Revised: 7 April 2014 – Accepted: 12 April 2014 – Published: 23 May 2014

Abstract. Atmospheric organic aerosols are generally classified as primary and secondary (POA and SOA) according to their formation processes. An actual separation, however, is challenging when the timescales of emission and gas-to-particle formation overlap. The presence of SOA formation in biomass burning plumes leads to scientific questions about whether the oxidized fraction of biomass burning aerosol is rather of secondary or primary origin, as some studies would suggest, and about the chemical compositions of oxidized biomass burning POA and SOA. In this study, we apply nuclear magnetic resonance (NMR) spectroscopy to investigate the functional group composition of fresh and aged biomass burning aerosols during an intensive field campaign in the Po Valley, Italy. The campaign was part of the EUCAARI project and was held at the rural station of San Pietro Capofiume in spring 2008. Factor analysis applied to the set of NMR spectra was used to apportion the wood burning contribution and other organic carbon (OC) source contributions, including aliphatic amines. Our NMR results, referred to the polar, water-soluble fraction of OC, show that fresh wood burning particles are composed of polyols and aromatic compounds, with a sharp resemblance to wood burning POA produced in wood stoves, while aged samples are clearly depleted of alcohols and are enriched in aliphatic acids with a smaller contribution of aromatic compounds. The comparison with biomass burning organic aerosols (BBOA) determined by high-resolution aerosol mass spectrometry (HR-TOF-AMS) at the site shows only a partial overlap between NMR BB-POA and AMS BBOA, which can be explained by either the inability of BBOA to capture all BB-POA composition, especially the alcohol fraction, or the fact that BBOA account for insoluble organic compounds unmeasured by the NMR. Therefore, an unambiguous composition for biomass burning POA could not be derived from this study, with NMR analysis indicating a higher O / C ratio compared to that measured for AMS BBOA. The comparison between the two techniques substantially improves when adding factors tracing possible contributions from biomass burning SOA, showing that the operational definitions of biomass burning organic aerosols are more consistent between techniques when including more factors tracing chemical classes over a range of oxidation levels. Overall, the non-fossil total carbon fraction was 50–57 %, depending on the assumptions about the ^{14}C content of non-fossil carbon, and the fraction of organic carbon estimated to be oxidized organic aerosol (OOA) from HR-TOF-AMS measurements was 73–100 % modern.

Published by Copernicus Publications on behalf of the European Geosciences Union.

1 Introduction

The adoption of new regulatory actions for reducing the emissions from fossil fuel combustion have certainly contributed to measurable decreases in atmospheric particulate matter concentrations in several areas in North America and Europe in the last two decades (Barmpadimos et al., 2011, 2012; Hand et al. 2012). This decreasing trend was flatter during the 2000s compared to the 1990s, in spite of the fact that emissions of sulfur, nitrogen and carbonaceous compounds from fossil fuel combustion have decreased steadily in Europe throughout the whole period (Harrison et al., 2008). Clearly, sulfate aerosols, whose reduction certainly boosted the PM10 reduction in Europe during the 1990s, are nowadays of secondary importance with respect to other aerosol components such as ammonium nitrate and organic aerosol (OA), which are becoming new targets. The evaluation of abatement strategies for the organic fraction of particulate matter is particularly challenging due to the number of anthropogenic and natural sources contributing to OA and to the complexity of the atmospheric processes controlling the concentrations of organic compounds susceptible to partitioning from the gas to the aerosol phase. There is actually no consensus on the best source apportionment method for particulate organic carbon (OC) and no single method would suffice, although important scientific achievements regarding its origin and atmospheric processing have been obtained in the last years. Some recent findings, relevant for the present study, are (a) the fact that a large fraction of modern carbon is found in OC, even in environments highly impacted by fossil fuel combustion (Hodzic et al. 2010); (b) the importance of residential biofuel combustion emissions worldwide, including industrialized countries (Bond et al., 2004; Kulmala et al., 2011); and (c) the fact that the budget of the OC emitted by combustion sources often includes a non-negligible fraction of secondary origin, i.e., forming in the plume by secondary reactions (Robinson et al. 2007; Nordin et al., 2013). These findings suggest that the presence of primary and secondary organic aerosol (respectively, POA and SOA) from biomass burning is much more significant than was believed in the past, and perhaps up to 30 % of the global aerosol OC budget (Hallquist et al., 2009).

In this study, we investigate the contribution of primary and secondary biomass burning to oxygenated organic aerosols in the rural Po Valley, Italy, in early spring: a period of the year during which diffuse wood burning from domestic heating systems is still active in the valley, and the meterorological conditions often favor stagnation of pollutants. In a previous paper (Saarikoski et al., 2012) we showed that under stable meteorological conditions the diurnal change in atmospheric stratification following the development of the planetary boundary layer was responsible for drastic changes in submicron aerosol composition, with fresh particulates rich in semivolatile compounds during the night and early morning, and more aged particles occurring in the middle of the day and in the afternoon. Atmospheric concentrations of particulate organic matter including fractions apportioned to biomass burning sources could be determined owing to the employment of an Aerodyne high-resolution time-of-flight mass spectrometer (HR-TOF-AMS, hereafter AMS) (De Carlo et al., 2006) and positive matrix factorization (PMF) analysis (Ulbrich et al., 2009). PMF analysis of AMS data sets provides factors for organic aerosol sources and corresponding contributions to OC concentrations. PMF is becoming common for organic source apportionment (Zhang et al., 2005; Lanz et al., 2007) and factor analysis of AMS data using PMF in its diverse implementations (including, e.g., ME-2) has extracted biomass burning organic aerosol (BBOA) factors at multiple sites (Aiken et al., 2010; Elsasser et al., 2012; Crippa et al., 2013a, etc.). Generally, the BBOA factors appear to reflect directly emitted primary biomass burning aerosol (p-BBOA), but the degree to which p-BBOA and secondary organic aerosol formed from biomass burning emissions are separated in PMF analyses has not been examined extensively.

Here we use ancillary information from tracer compounds, some of which are already included in the study of Saarikoski et al. (2012), and other spectroscopic techniques suitable for organic source attribution, presented here for the first time, such as nuclear magnetic resonance (NMR) spectroscopies (Hallquist et al., 2009) to investigate the separation of primary and secondary biomass burning-related emissions during the Po Valley spring measurements. Proton NMR (^{1}H-NMR) spectroscopy in particular has already been used successfully to characterize biomass burning aerosols in tropical environments (Decesari et al., 2006), and has also been proposed as a tool for source attribution of water-soluble organic aerosol including biomass burning particles (Decesari et al., 2007). In this paper, we compare the spectral fingerprints of wood burning aerosol as determined by HR-TOF-AMS and ^{1}H-NMR spectroscopies during the 2008 EUCAARI experiment in the Po Valley, and we interpret the chemical composition of NMR-determined biomass burning aerosol on the basis of laboratory and field data obtained in past and parallel experiments.

2 Experimental

2.1 The 2008 EUCAARI Po Valley campaign

The measurements were conducted at the G. Fea (44°39′0″ N, 11°37′0″ E; Decesari et al., 2001) San Pietro Capofiume (SPC) measurement station from 30 March to 20 April 2008. The station is located about 30 km northeast of the city of Bologna in an area of the Po Valley open to the Adriatic Sea on the eastern side, but surrounded by densely populated areas on its southern, western and northern sides. The station of San Pietro Capofiume belongs to the ARPA-ER (Agenzia Regionale

Prevenzione e Ambiente – Emilia-Romagna) network for meteorological observations and air quality monitoring. The station regularly hosts measurements of aerosol chemical and physical measurements and aerosol optical properties and light extinction run by ISAC-CNR, ARPA-ER and the University of Eastern Finland. During the 2008 EUCAARI experiment, a suite of additional aerosol measurements was implemented including AMS (Saarikoski et al., 2012), HTDMA and air ion spectrometers (Manninen et al., 2010).

On the basis of the meteorological conditions and back-trajectory analysis, five periods can be distinguished: Period I (30 March to 6 April) characterized by vertical atmospheric stability, relatively low wind speeds (2.4 m s^{-1} on average), high pollution levels and marked diurnal variations in aerosol concentration and composition; Period II (7 April) with low concentrations and significant transport from outside the valley, suggested also by the highest mean wind speed of the campaign (4.3 m s^{-1} on average); Period III (8 to 11 April) with re-established stable conditions, lower wind speed (1.9 m s^{-1} on average), high pollution levels, high humidity, little diurnal variations and transport of maritime air masses; Period IV (April 11 and 12) characterized by atmospheric instability, again higher wind speed (3.2 m s^{-1} on average) and very low aerosol concentrations; Period V (12 to 20 April) with high variability (with wind speeds ranging between 0.2 and 6.9 m s^{-1}), intermittent precipitation events and moderate average pollutant concentrations. The PM1 chemical composition observed during the five periods reflected the different meteorological and atmospheric transport conditions, with higher concentrations of ammonium nitrate during the polluted days and greater proportions of ammonium sulfate in background conditions (Saarikoski et al., 2012), in line with behavior typical of many continental environments.

2.2 Sampling and off-line chemical analysis

A dichotomous sampler (Universal Air Sampler, model 310, MSP Corporation) at a constant nominal flow of 300 l/min was employed from 1 to 14 April 2008 to collect fine particles with ambient diameter < 1 µm on pre-washed and pre-baked quartz-fiber filters (Whatman, Ø = 9 cm). Typically, two filters were sampled every day: a "daytime" (D) PM_1 sample was collected from ∼10:00 to ∼17:00 (local time, UTC+2) followed by an "evening/night-time" (N) sample collected from ∼18:00 to ∼09:00. Exceptionally, long-time integrated samples ($n = 3$, lasting 32, 24 and 24 h) were taken using an Andersen PM10 high-volume (HiVol) sampler at critical flow (1.13 m^3 min^{-1}) equipped with quartz-fiber filters (Whatman, 8 × 10 in.). All samples were stored frozen until chemical analysis.

Total carbon (TC) content was measured directly from small sub-samples of the quartz-fiber filters (1 cm^2) by evolved gas analysis. Measurements were performed by a multi N/C 2100 analyzer (Analytik Jena, Germany) equipped with a module for solid samples. Samples were oxidized in an atmosphere of pure oxygen and by applying a temperature ramp (up to 950 °C). TC was measured as total evolved CO_2 by a non-dispersive infrared (NDIR) analyzer (Gelencser et al., 2000).

The remaining portion of each filter was extracted with deionized ultra-pure water (Milli-Q) in an ultrasonic bath for 1 h and the water extract was filtered on PTFE membranes (pore size: 0.45 µm) in order to remove suspended particles. Aliquots of the water extracts were used to determine the water-soluble organic carbon (WSOC) content by a multi N/C 2100 total organic carbon analyzer (Analytik Jena, Germany) using the interface for liquid sample injection. The analysis provided the WSOC concentration in the extracts upon correction for the inorganic carbon (carbonate) concentration (Rinaldi et al., 2007). The difference between TC and WSOC and carbonate carbon resulted in the water-insoluble carbon (WINC), which accounts for insoluble organic compounds plus elemental carbon.

Concentrations of major inorganic ions (NH_4^+, Na^+, K^+, Ca^{2+}, Mg^{2+}, Cl^-, NO_3^-, SO_4^{2-}) and some organic acids (i.e., oxalate) were determined in the water extracts of the PM1 filters by ion chromatography (IC) using the same protocol adopted for the Berner impactor samples analyzed in the same experiment (Saarikoski et al., 2012).

The remaining aliquots of the water extracts were dried under vacuum and re-dissolved in deuterium oxide (D_2O) for functional group characterization by proton nuclear magnetic resonance (^{1}H-NMR) spectroscopy (Decesari et al., 2000). The extracts of the seven samples collected during periods IV and V of the campaign were lumped into three samples to increase the sample load and sensitivity of the analysis. The ^{1}H-NMR spectra were acquired at 400 MHz with a Varian Mercury 400 spectrometer in a 5 mm probe. Sodium 3-trimethylsilyl-(2,2,3,3-d4) propionate (TSP-d4) was used as the referred internal standard, adding 50 µl of a TSP-d4 0.05 % (by weight) solution in D_2O (1.5 µmolH belonging to the standard in the probe). ^{1}H-NMR spectroscopy in protic solvents provides the speciation of hydrogen atoms bound to carbon atoms. On the basis of the range of frequency shifts (the chemical shift, ppm) in which the signals occur, they can be attributed to different H–C-containing functional groups. Detection limits for an average sampling volume of 500 m^3 were on the order of 3 nmol m^{-3} for each functional group.

Since aliphatic carbonyls or carboxylic groups do not have detectable protons, their concentrations can be detected by proton NMR spectroscopy only indirectly, on the basis of the intensity of resonances between 1.9 and 3.0 ppm of chemical shift, which can be attributed to aliphatic groups adjacent to an unsaturated carbon atom, e.g., HC–C=O, HC–COOH or HC–C=C. Since aromatic and vinyl groups are relatively scarce in WSOC atmospheric samples, the unsaturated oxygenated groups provide the greatest contribution. The approach of Decesari et al. (2007) includes a correction for the

contribution of benzylic groups (CH–Ar), which is assumed to be proportional to the total aromatic protons and is subtracted from total H–C–C= moieties to derive the aliphatic groups containing oxygenated unsaturated groups (i.e., carbonyls and carboxyls), HC–C=O.

Recent works (Tagliavini et al., 2006; Moretti et al., 2008) introduced a methodology for direct determination of carbonyls and carboxylic groups by coupling chemical derivatization to proton NMR spectroscopy, and which was applied to the present study. Briefly, carboxylic acids were converted to methyl-esters by reaction with diazomethane and the concentration of the products was quantified by integrating the band between 3 and 4 ppm in the ^{1}H-NMR spectrum after subtraction of the signals of the underivatized sample. An analogous procedure was applied for carbonyls, which were derivatized to methyloximes by reaction with O-methyl-hydroxylamine. A detailed discussion of the methodology is presented in Moretti et al. (2008). The chemical derivatization procedure is labor intensive and, in its current version, is not designed for the analysis of a large number of samples. In this study it was employed at an explorative level mainly to probe the oxygenated functional group distribution information. The advantages of chemical derivatization – NMR analysis as a benchmark methodology for fast AMS measurement are the specificity of functional group derivatization and the "soft", non-destructive NMR detection.

An anion-exchange high-performance liquid chromatography (HPLC-TOC) technique already described by Mancinelli et al. (2007) was also employed on one aerosol sample collected during the EUCAARI field campaign. The technique, based on a purely inorganic buffer, allows the fractionation of WSOC into four chemical classes, namely neutral/basic compounds (NB), mono-acids (MA), di-acids (DA) and poly-acids (PA, representative of humic-like substances), and their quantification by off-line TOC analysis. The same multi N/C 2100 total organic carbon analyzer used for total WSOC analysis was also employed for analysis of the chromatographic fractions.

2.3 Factor analysis of NMR spectra

Factor analysis (FA), in the broad sense, includes several multivariate statistical techniques that have been extensively used in the last years in atmospheric sciences for aerosol source apportionment on the basis of the internal correlations of observations at a receptor site, or receptor modeling (Viana et al., 2008). Regardless of the specific constraints imposed and the different algorithms, all the different methods of FA are based on the same bilinear model that can be described by Eq. (1):

$$x_{ij} = \sum_{k=1}^{p} g_{ik} f_{kj} + e_{ij}, \quad (1)$$

where x_{ij} refers to a particular experimental measurement of concentration of species $\boldsymbol{j}$ (one of the analytes or, here, one point of the mass or NMR spectrum) in one particular sample $\boldsymbol{i}$. Individual experimental measurements are decomposed into the sum of $\boldsymbol{p}$ contributions or sources, each one of which is described by the product of two elements, one (f_{kj}) defining the relative amount of the considered variable j in the source composition (loading of this variable on the source) and another (g_{ik}) defining the relative contribution of this source in that sample i (score of the source in this sample). The sum is extended to $k = 1,\ldots, p$ sources, leaving the unexplained residual stored in e_{ij}.

The application of factor analysis techniques to NMR spectral data sets is relatively new for atmospheric sciences, though being widely employed in other fields, especially in biochemistry. The most simple techniques suitable for 1-D spectra allow for deconvolution into spectral profiles (loadings) and corresponding contributions (scores). In the present study, we employed FA to analyze the collection of 17 NMR spectra of ambient samples collected during the EUCAARI campaign, and to identify and quantify major components of WSOC. The NMR data were processed following the method described below.

The rough NMR spectra were subjected to several preprocessing steps prior to undergoing FA in order to minimize spurious sources of variability. A polynomial fit was applied to the baselines and subtracted from the spectra. After a careful horizontal alignment of the spectra (with the Tsp-d4 singlet set at chemical shift $\delta H = 0$), the peaks overlapping with blank signals were removed. The spectral regions containing only sparse signals ($\delta H < 0.5$ ppm, $4.5 < \delta H < 6.5$ ppm, and $\delta H > 8.5$ ppm) were omitted. Binning over 0.02 ppm chemical shift intervals was applied to remove the effects of peak position variability caused by matrix effects. Low-resolution (400-point) spectra were finally obtained. The factor analysis methods used in this study include non-negative matrix factorization (N-NMF) and multivariate curve resolution (MCR), which are among the most common NMR spectral unmixing techniques in many chemometric applications (Karakach et al., 2009). Two different algorithms were used for NMF, employing a projected gradient bound-constrained optimization (Lin, 2007) or a multiplicative update approach (Lee and Seung, 2001). Finally, MCR was run according to two different algorithms: the classical alternating least squares approach (MCR-ALS, Tauler, 1995; Jaumot et al., 2005) and a weighted alternating least squares method (MCR-WALS, Wentzell et al., 2006). The mathematical goal of every model is to find the values of g_{ik}, f_{kj} and p that best reproduce x_{ij}. For this purpose the values of g_{ik} and f_{kj} are iteratively fitted to the data using a least squares algorithm, minimizing the fit parameter called Q. Q may be defined in different ways depending on the model's approach, but it is substantially always the sum of squared residuals:

$$Q^2 = \sum_{i=1}^{m} \sum_{j=1}^{n} \left(x_{ij} - g_{ik} \cdot f_{kj}\right)^2 \quad (2)$$

Unlike the classic PMF that requires an error matrix as input because its object function Q weighted the residuals by their respective uncertainties, NMF and MCR methods do not require any term referred to uncertainty and the Q value depends only on the difference between the measurements (x_{ij}) and the model's results ($g_{ik} \cdot f_{kj}$).

2.4 Wood burning emission experiments

A rather modern log-wood stove described in Heringa et al. (2011) was operated to sample domestic wood burning emission samples for later NMR analysis. A Dekati dilution system was used to dilute the exhaust by around a factor of 8. The flow directed on the filter was 10 liters per minute. The filters were sampled over 90 min and included the starting of the fire, a rather long flaming phase (with several add-ons of beech logs) and one smoldering phase at the end.

2.5 Isotopic measurements

Measurements of ^{14}C were performed on total carbon (TC) aerosols on 12 samples to obtain further source information (fossil or modern origin). The ^{14}C methodology is based on the fact that aerosols of fossil origin are completely depleted in ^{14}C due to their age, while aerosols originating from non-fossil sources (e.g., biogenic sources and biomass combustion) contain a $^{14}C/^{12}C$ ratio that can be estimated from recent atmospheric ^{14}C values. In brief, each filter sample, containing 50–80 µg of carbon, was combusted to CO_2 in a vacuum system in the presence of pre-cleaned CuO needles (1 g; Merck pro analysis, 0.65 × 6 mm) (Genberg et al, 2010; Genberg et al, 2011). After purifying the evolved CO_2 cryogenically, the gas was mixed with H_2 and reduced to solid carbon using an iron catalyst at 600 °C (1 mg Fe, Merck, pro analysis, reduced, diameter 10 µm). $Mg(ClO_4)_2$ (Merck, diameter 1–4 mm) was used as a drying agent. After the reduction step (complete reaction time < 4 h) the carbon and iron catalysts were pressed into an aluminum sample holder. The sample holders containing the carbon from the aerosol samples were placed on a 40-position sample wheel together with graphitized standards (4 IAEA-C6 as the primary standard; 4 IAEA-C7 and 2 OxI as the secondary standards) and blanks (four samples produced from bottled, commercial fossil CO_2). The ^{14}C analysis was performed using the single stage accelerator mass spectrometry (SSAMS) facility at Lund University (Skog, 2007; Skog et al., 2010).

The results from the ^{14}C measurements are expressed as a "fraction of modern carbon" ($F^{14}C$) (Reimer et al., 2004). Carbon originating from fossil sources has a $F^{14}C$ value of 0. A $F^{14}C$ value of 1.0 represents a hypothetical concentration of naturally produced ^{14}C in atmospheric carbon from 1950, excluding anthropogenic influences. However, the atmospheric ^{14}C concentration has been altered due to emissions of fossil CO_2 (the Suess effect: decreasing the ^{14}C concentration) and due to the formation of ^{14}C from testing of nuclear weapons in the late 1950s and early 1960s (the bomb effect: increasing the ^{14}C concentration). Due to the latter effect, the $F^{14}C$ value of atmospheric carbon dioxide in the Northern Hemisphere reached a maximum value of almost 2.0 in 1963. After the Limited Test Ban Treaty, signed in 1963, atmospheric ^{14}C began to decrease quickly, mainly due to the transfer of atmospheric carbon into oceans and the biosphere. In 2008, $F^{14}C$ has dropped to about 1.04 (see Genberg et al., 2011, and references therein). This value is representative of biogenic sources of carbon in 2008 and will be used in the next discussion (Sect. 5) as a "reference fraction of modern carbon of biogenic aerosol" (or fM(bio)). For periods dominated by biomass burning aerosol, assumptions have to be made regarding the average age of the biomass because due to the older age of burnt wood carbonaceous aerosol from biomass burning is more enriched in ^{14}C than biogenic aerosol associated with primary biological particles (PBAP) and biogenic SOA. In the Genberg et al. (2011) paper a 60 to 80 year old tree harvested in 2008 has a $F^{14}C$ value of between 1.21 and 1.23. However, according to Gilardoni et al. (2011), the most probable $F^{14}C$ value for aerosols from biomass combustion in the Po Valley is 1.19. Hence this value was used here as a "reference fraction of modern carbon of biomass burning aerosol" (or fM(bb)). Results of this analysis and correction of the data will be further discussed below in Sect. 5.

3 Results of the chemical analyses

3.1 Overview

Spring is a transition season in northern Italy, with variable weather conditions and frequent precipitation. The highest aerosol concentrations in the Po Valley region are typically found in the cold season when the atmosphere is more stably stratified. However, on four days among the twenty-one of the EUCAARI campaign, PM10 concentrations exceeded the 50 µg m^{-3} threshold at more than one ARPA-ER station within a set of thirteen located in an area of 100 km around San Pietro Capofiume. On 9 and 10 April, ten stations showed concentrations above 40 µg m^{-3}. These kinds of pollution events extending over an entire sector of the Po Valley provide an example of how distributed pollution sources associated with a particular orography and under stagnant meteorological conditions lead to regional pollution events characterized by small differences in aerosol loadings between urban and rural environments. The same small differences between urban and rural areas have also been observed around Paris (Crippa et al., 2013b; Freutel et al., 2013) and Barcelona (Minguillón et al., 2011), indicating that this is probably rather common in the whole European domain.

During the first week of high-pressure conditions, the concentrations of NO_x and the non-refractory submicron aerosol components measured by the AMS exhibited sharp

diurnal trends, with maxima during the night and early morning (Saarikoski et al., 2012). Such behavior is characteristic of primary or freshly produced compounds accumulating in the surface layer under a low thermal inversion and being dispersed upon formation of the mixing layer in the late morning. The HR-TOF-AMS results showed that ammonium nitrate and several of the organic fractions identified by positive matrix factorization (PMF) followed diurnal variations, while ammonium sulfate and the most oxidized fraction of particulate organic compounds ("OOA-a" in Saarikoski et al., 2012, but referring to the so-called OOA-1 or LV-OOA in previous literature) showed no variations, pointing to components well mixed in the lower troposphere and therefore not linked to local sources in the Po Valley (Saarikoski et al., 2012). Among the organic fractions identified, some exhibited a low O / C ratio, namely HOA (hydrocarbon-like compounds) that are influenced by traffic emissions, BBOA (biomass burning organic aerosols) and N–OA (nitrogen-containing organic aerosols). The above three classes of organics showed diurnal trends, with minima in afternoon hours and with more or less pronounced maxima in early morning or evening hours. Finally, two classes of oxygenated species, OOA-b and -c, had an oxygen-to-carbon ratio intermediate between that of BBOA and that of OOA-a, and showed complex diurnal trends. In addition, OOA-c was linked to biomass burning sources based on its downward trend in concentration observed during the campaign and based on its correlation with anhydrosugars.

In this paper we compare the AMS concentrations for particulate organic compounds with those derived by off-line thermal (EGA, liquid TOC) and ^{1}H-NMR analyses. Since the three techniques employ different units (μg/m^3 of organic matter, organic carbon and organic hydrogen, respectively), stoichiometric ratios must be applied for quantitative comparison. In the following discussion, all concentrations of AMS factors for organic matter will be converted (using the OM / OC and H / C ratios reported by Saarikoski et al. (2012)) to μg m^{-3} of organic carbon (μgC m^{-3}) for comparison with thermal analyses, and organic carbon and organic hydrogen for comparison with the NMR spectroscopic data. The NMR concentrations for functional groups will be reported in μmolH m^{-3}, or upon conversion into μgC m^{-3} by assuming the group-specific H / C ratios introduced in previous studies (Decesari et al., 2007).

A quantitative comparison between AMS- and NMR-detected oxidized organic compounds necessitates an examination of possible biases between the total particulate organic material sampled by the filters and measured by the AMS. During the Po Valley campaign the collection efficiency (CE) of the AMS was determined based on a comparison with co-located off-line chemical measurements: Saarikoski et al. (2012) discussed more extensively the criteria applied for the CE estimation in order to correct a systematic underprediction in absolute AMS mass concentration that occurred during the first portion of the campaign (before 9 April); here we compare AMS measurements with the PM1 filters collected with the dichotomous sampler and not included in the analysis of Saarikoski et al. (2012). Unfortunately, only TC and not the OC / EC split was available for the PM1 filters, but assuming the average EC fraction (EC / TC = 25 %) determined on a set of filters taken in parallel (Saarikoski et al., 2012), the ratio between the total AMS organic compounds, expressed in μgC m^{-3}, and the total OC measured on the filters was 0.97 ± 0.30 ($n = 17$, $R = 0.87$), indicating no clear positive or negative biases between the two measurement systems. In previous studies (Kondo et al., 2007) water-soluble organic carbon (WSOC) was attributed completely to AMS OOAs, while water-insoluble organics were apportioned to HOA. In the Po Valley, we also had a good correlation between the organic carbon accounted for by the AMS OOA factors and the WSOC determined on the filters ($AMS_{(OOAs+N-OA)}$ / FiltersWSOC slope = 0.97). A slightly greater slope (1.15) is obtained when including the BBOA among the AMS factors contributing to the water-soluble aerosol (Fig. 1a). The average AMS/filter ratios were 0.79 and 0.90 for the two cases, suggesting that BBOA could contribute to WSOC, with only HOA being apportioned to the water-insoluble fraction, in agreement with the findings of Kondo et al. (2007). Overall, the correlation between the WSOC measured on filters and that derived from the AMS factors containing heteroatoms was positive but quite scattered ($R \sim 0.77$). When comparing the AMS oxygenated or nitrogenated organic carbon with the WSOC speciated by the NMR analysis, we found a 20 % excess in the AMS concentration when considering BBOA water soluble. This can be explained by the incomplete NMR characterization of the total WSOC, with an average ratio between NMR and liquid-TOC analysis of 0.75 ± 0.14 ($n = 17$, $R = 0.92$). This finding is in line with previous NMR measurements (Tagliavini et al. 2006), although lower with respect to the results obtained during other EUCAARI field experiments in European polluted environments (manuscript in preparation). Likely sources of missing carbon are compounds not carrying non-exchangeable hydrogen atoms, like oxalic acid, and volatile components present in WSOC originating from positive artefacts or from the hydrolysis of oligomers of low-molecular-weight compounds and lost during sample preparation. Another source of uncertainty is the stoichiometric H / C ratios applied to the ^{1}H-NMR functional groups and that may underestimate structures having low hydrogen content. For this reason, the NMR/AMS comparison was also carried out employing *organic hydrogen concentration units* (Fig. 1d), which are determined directly by the NMR analysis without the need for any conversion factors, while the AMS data are derived by applying the H / C ratios estimated by high mass resolution analysis (Saarikoski et al., 2012). Fig. 1d shows again an excess of concentration in the AMS data with respect to NMR, greater for hydrogen than for carbon. This indicates that the non-exchangeable organic hydrogen determined by proton-NMR is a fraction of the total

Table 1. Concentrations (ng m^{-3}) of alkyl amines as measured by ^{1}H-NMR spectra.

	MMA	DMA	TMA	TEA
Period I ($n = 7$)	3	6	2	3
Period III ($n = 6$)	5	8	1	30
Periods II, IV and V ($n = 4$)	1	3	1	6
All campaigns	3	6	1	13

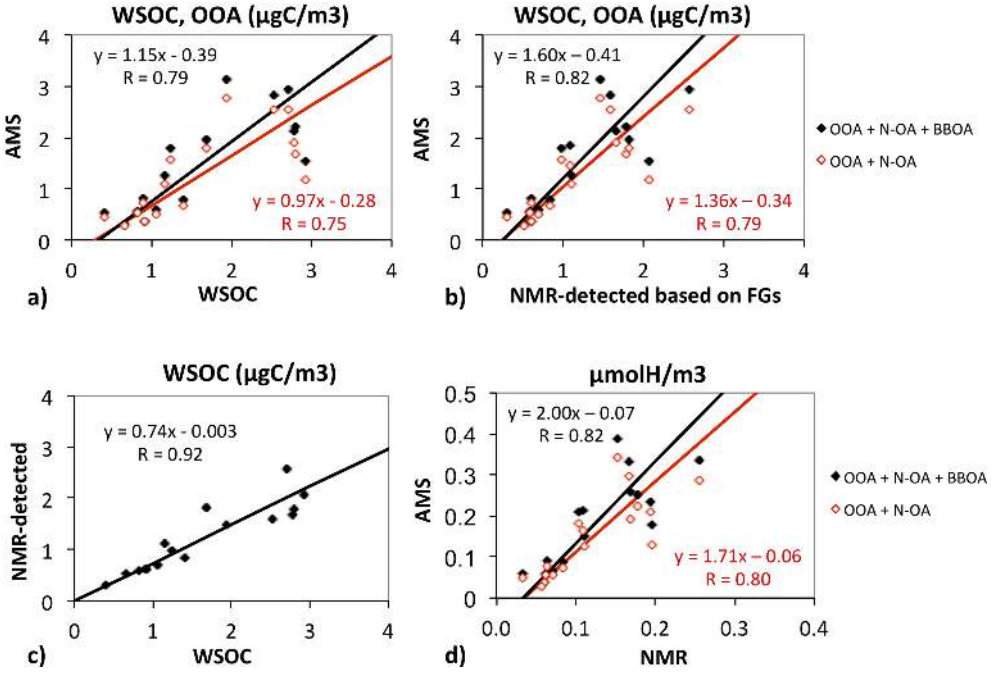

Figure 1. (a), **(b)**, **(c)** Orthogonal fitting between carbon classes derived from TOC analysis, AMS measurements and ^{1}H-NMR analysis. **(d)** Scatter plot (with orthogonal linear fit again) between AMS and ^{1}H-NMR concentrations of organic hydrogen.

hydrogen atoms detected by AMS, and therefore the AMS – unlike NMR – accounted for at least some of the acidic hydrogen atoms of H–O bonds in alcohols and carboxylic acids.

3.2 NMR characterization of WSOC

Figure 2 shows examples of ^{1}H-NMR spectra recorded during the 2008 EUCAARI experiment in the Po Valley. Spectral fingerprints and individual compound speciation are in agreement with previous findings in the same area (Decesari et al., 2001). Levoglucosan, methane–sulfonate and four low molecular weight amines, namely monomethyl-, dimethyl-, trimethyl- and triethyl-amines (MMA, DMA, TMA, TEA), were speciated and quantified. Contrary to the marine aerosol samples collected on the Irish coast (Decesari et al., 2011), diethyl-amine (DEA) was not found, while TMA and TEA were detected at the ng m^{-3} level in almost all samples (Table 1). The different speciation with respect to the marine site probably reflects different biogenic sources, which in the Po

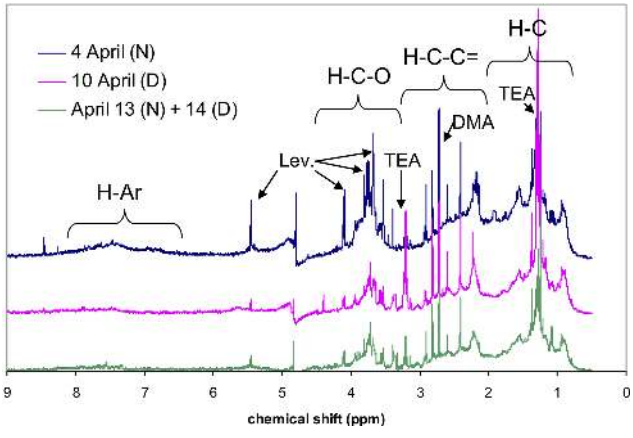

Figure 2. Examples of ^{1}H-NMR spectra of different aerosol SPC 2008 EUCAARI samples.

Table 2. Average functional group concentrations as nmolH m^{-3} and µgC m^{-3} in the different periods of the campaign and for the whole experiment.

	nmol H m^{-3}						µgC m^{-3}						
	H–Ar	H–C–O	MSA	HC–N	H–C–C=	H–C	H–Ar	H–C–O	MSA	HC–N	H–C–(C=)	(H–C)–C=O	H–C
Period I ($n = 7$)	7.9	16.0	0.3	1.6	36	42	0.24	0.17	0.00	0.01	0.21	0.17	0.25
Period III ($n = 6$)	5.5	16.2	0.9	3.5	38	55	0.17	0.18	0.00	0.02	0.23	0.20	0.33
Periods II, IV and V ($n = 4$)	2.1	7.3	0.3	1.0	19	29	0.06	0.08	0.00	0.01	0.11	0.10	0.17
All campaigns	5.7	14.0	0.5	2.2	33	43	0.17	0.15	0.00	0.01	0.20	0.17	0.26

Valley are largely impacted by livestock farming and waste treatment activities (Ge et al. 2011). Wood burning is an additional source of amines in the valley, but the correlations with levoglucosan concentrations are negligible for most of them. With the exception of TMA, whose time trend is rather flat, the other amine concentrations reach a maximum in the third period of the campaign, on the days between 8 and 10 April, characterized by western Mediterranean air masses, high humidity with fog occurrence and a very stratified atmosphere. We observed the highest concentrations of ammonium nitrate in the same period, indicating that the high relative humidity may have promoted the gas-to-particle conversion of low-molecular-weight amines by co-condensation with nitric acid or organic acids.

A summary of the WSOC functional group distribution is provided in Table 2, while a synthetic representation of its variability during the campaign is provided by Fig. 3, based on the metrics introduced by Decesari et al. (2007). Briefly, the aliphatic composition of the samples is defined by two variables: the proportion of alkoxy groups (H–C–O) and that of aliphatic groups functionalized with carbonyls or carboxyls (H–C–C=O). In addition, the ratio between NMR-detected aromatic vs. aliphatic groups is visualized by dot size. Functional group concentrations are expressed here as µgC m^{-3} upon applying group-specific conversion factors introduced in the paper above. Regions of the diagram assigned to broad WSOC categories, namely SOA, biomass burning aerosol and marine aerosol, were identified on the basis of characterization of near-source samples (Decesari et al. 2007). With the aim of comparison we plotted the composition of the Po Valley samples discussed in Decesari et al. (2001) or collected during other experiments (unpublished data) before the 2008 EUCAARI campaign. The 2008 spring campaign samples exhibit an aliphatic composition stretching between the biomass burning and SOA sectors, with a prevalence of the latter. A clear biomass burning assignment was found for samples 04April_Night and 05April_Night, meaning that their composition is fully consistent with that recorded for samples taken in an area (Rondônia, Brazil) exposed directly to strong biomass burning emissions (Tagliavini et al. 2006).

The aromaticity of WSOC, defined again as the ratio between NMR-detected aromatic vs. aliphatic groups, decreased steadily during the campaign (Fig. 3b) with a trend already observed for anhydrosugars and that can be explained by the progressive increase in minimum temperatures leading to a general decline in residential heating activities in the area (Saarikoski et al., 2012). This finding suggests that NMR-detected aromatics are mainly phenolic compounds formed by the pyrolysis of wood during combustion, together with their degradation products in the atmosphere.

The proportion of alkyl groups to the aliphatic moieties remains fairly constant, resulting in a certain degree of covariance between the two main oxygenated groups, H–C–O and H–C–C=O. The conversion between hydroxylated compounds and those bearing carbonyls/carboxyls seems to be related to the air mass type and photochemical regime, since there is a clear tendency to find the former at high O_3 / NO_2 ratios and the latter in more photochemically aged air masses (Fig. 3c). It should be noted that the actual change in the WSOC oxidation state as a consequence of the "replacement" of hydroxyl-functional groups with H–C–C=O groups cannot be determined accurately based on these data, due to the uncertainty in the split between carbonyls and carboxylic groups. Examples of how such speciation can be reached using proton NMR techniques are presented in the following section.

3.3 Carbonyl and carboxylic acid concentrations by NMR and AMS

With the aim of a direct determination of carbonyls and carboxylic groups by proton NMR spectroscopy, a total of five Andersen PM10 HiVol sample extracts, one night time and four day time, underwent chemical derivatization for carbonyl and carboxylic acid determination following the chemical derivatization procedures described in Sect. 2.2. Carbonyl and carboxylic acid concentrations determined with

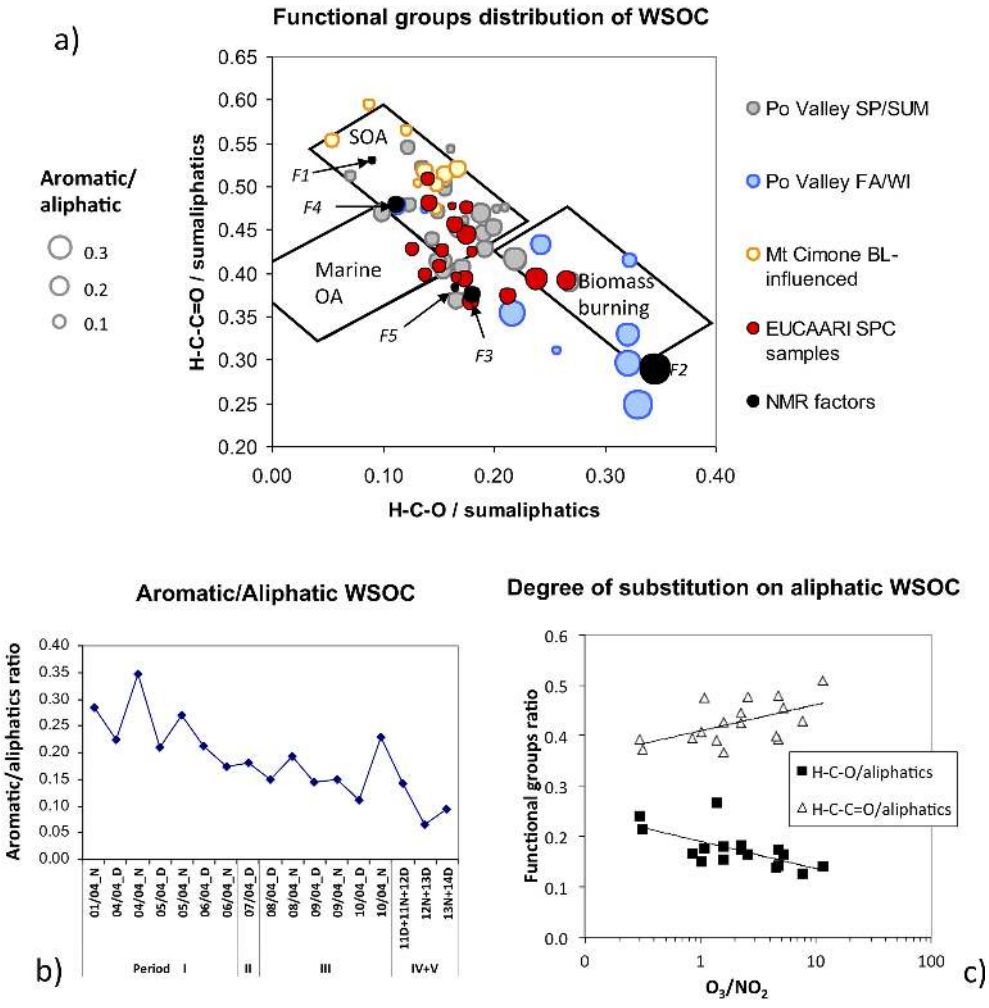

Figure 3. **(a)** ^{1}H-NMR functional group distribution of the SPC 2008 EUCAARI samples compared to submicron aerosol compositions derived from previous studies in the same area. Black dots represent the functional group distribution of the NMR factors derived from the factor analysis described in the following Sect. 3.4. **(b)** Time trend of aromaticity (defined as the ratio between aromatics and the sum of aliphatic groups). **(c)** Relative content of oxygenated aliphatic functional groups as a function of trace gas composition.

Table 3. COOH and carbonyl concentrations from AMS and derivatization – ^{1}H-NMR analysis. All concentrations in μgC m^{-3}. AMS OOC stands for the carbon concentrations of all OOA types and BBOA.

	NMR			AMS		
Sample	WSOC	COOH	C=O	OOC	fragment CO_2^+	fragment $C_2H_3O^+$
31/03_N	2.15	0.10	0.13	2.93	0.26	0.069
14/04_D	1.36	0.05	0.08	0.55	0.092	0.019
16/04_D	1.17	0.07	0.06	0.79	0.098	0.025
17/04_D	1.22	0.15	0.06	0.91	0.11	0.028
19/04_D	1.32	0.08	0.10	1.27	0.16	0.06

NMR were also compared with AMS measurements of fragments m/z 43 ($C_2H_3O^+$) and 44 (CO_2^+) in the corresponding time periods: in fact, although we acknowledge that an exact relationship between these signals and carbonyl and carboxylic acid concentration has not yet been established clearly (Duplissy et al., 2011 have established a relationship for mono- and di-acids only), we use here CO_2^+ and $C_2H_3O^+$ as proxies for acid and non-acid oxygenated functional groups, respectively. Concentrations of both functional groups from NMR derivatization ranged from 0.05 to

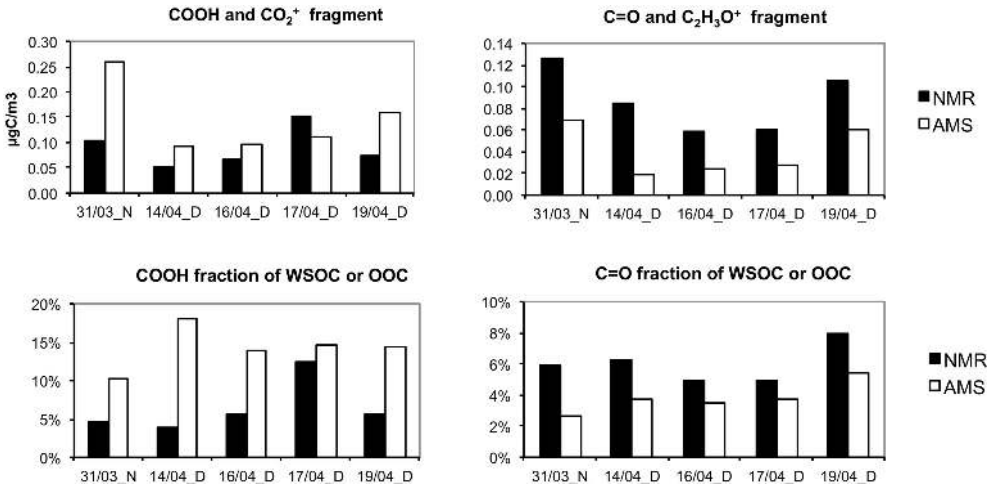

Figure 4. Concentration of carboxylic acids and carbonyls determined by chemical derivatization – ^{1}H-NMR analysis in five PM1 WSOC samples. Time-averaged concentrations of the CO_2^+ and $C_2H_3O^+$ fragments from HR-TOF-AMS measurements are also reported as proxies for acid and non-acid oxygenated functional groups, respectively. For more details refer to the text.

0.15 µgC m^{-3} (4 to 10 nmol m^{-3}), which is the same order of magnitude derived from the AMS measurements (Table 3). However, the carboxylic acid concentrations determined by the NMR method are lower than those from AMS in most cases (Fig. 4) and their correlation is not good ($R = 0.19$). Such a discrepancy could be explained by the unavoidable loss of volatile carboxylic acids during the chemical derivatization procedure, or by the formation of CO_2^+ fragments in the AMS vaporizer from groups other than carboxylic acids, like esters and peroxides. An analogous comparison for the carbonyls shows a better correlation ($R = 0.87$) between the concentrations determined by the two techniques, although the NMR methodology provides higher absolute values and slightly higher proportions to WSOC or OOA carbon (Fig. 4), suggesting that the $C_2H_3O^+$ fragments in the AMS spectra do not represent the totality of carbonyls (which might produce other fragments, i.e., CHO^+), although they certainly account for the largest part of them.

3.4 NMR factor analysis

Four methods of factor analysis (two NMF and two MCR) were applied to the series of 17 ^{1}H-NMR spectra at 400-point resolution (see Sect. 2.3). Solutions with a number of factors of 2 up to 8 were explored. The five-factor solution showed the best agreement between the four algorithms in respect to both spectral profiles and contributions. With a greater number of factors, strong correlations between two or more factors are found (Table S1), suggesting that the measurements were not adequate for differentiating additional independent factors. This is also confirmed by the analysis of the dependence of the Q values on the factor number, showing a marked drop until a number of five and flattening out at greater numbers of factors (Fig. S1). For more details on the criteria used for choosing the factor number in NMR factor analysis see also the supplementary material.

Figure 5 reports profiles and contributions of the five-factor solution resulting from the four algorithms. The interpretation of factor spectral profiles was based on the presence of molecular resonances of tracer compounds, and on the comparison with a library of reference spectra recorded in the laboratory or in the field during near-source studies. The physical nature of the factors was also interpreted on the basis of correlation analysis employing atmospheric tracers (Table 4).

– NMR Factor 1 (F1: "MSA-containing") exhibits the resonance of methane–sulfonic acid (MSA) at 2.81 ppm as the most characteristic peak. The peak overlaps with a background signal attributable to oxidized aliphatic chains. F1 air concentrations were low during the campaign, varying from ∼0.00 to 0.02 µgCm^{-3}, reaching 0.06 µgCm^{-3} on the night of 4 April. MSA is generally considered a marker for marine SOA, and its occurrence in the Po Valley can be explained by the proximity of the sea. This interpretation is supported by back-trajectory analysis, showing that during Period III of the campaign, when the highest concentration of F1 was observed, westerly humid air masses that had travelled over the western Mediterranean Sea reached the Po Valley. In the same period, however, atmospheric stratification promoted the increase of pollutants originating from land sources. Possible contributions of continental sources to MSA include the emissions of organic sulfur from animal husbandry and landfilling (e.g., Kim 2006), especially from pig farms, which are particularly diffused in the Po Valley. However, the correlation of MSA with other tracers of emissions from anaerobic

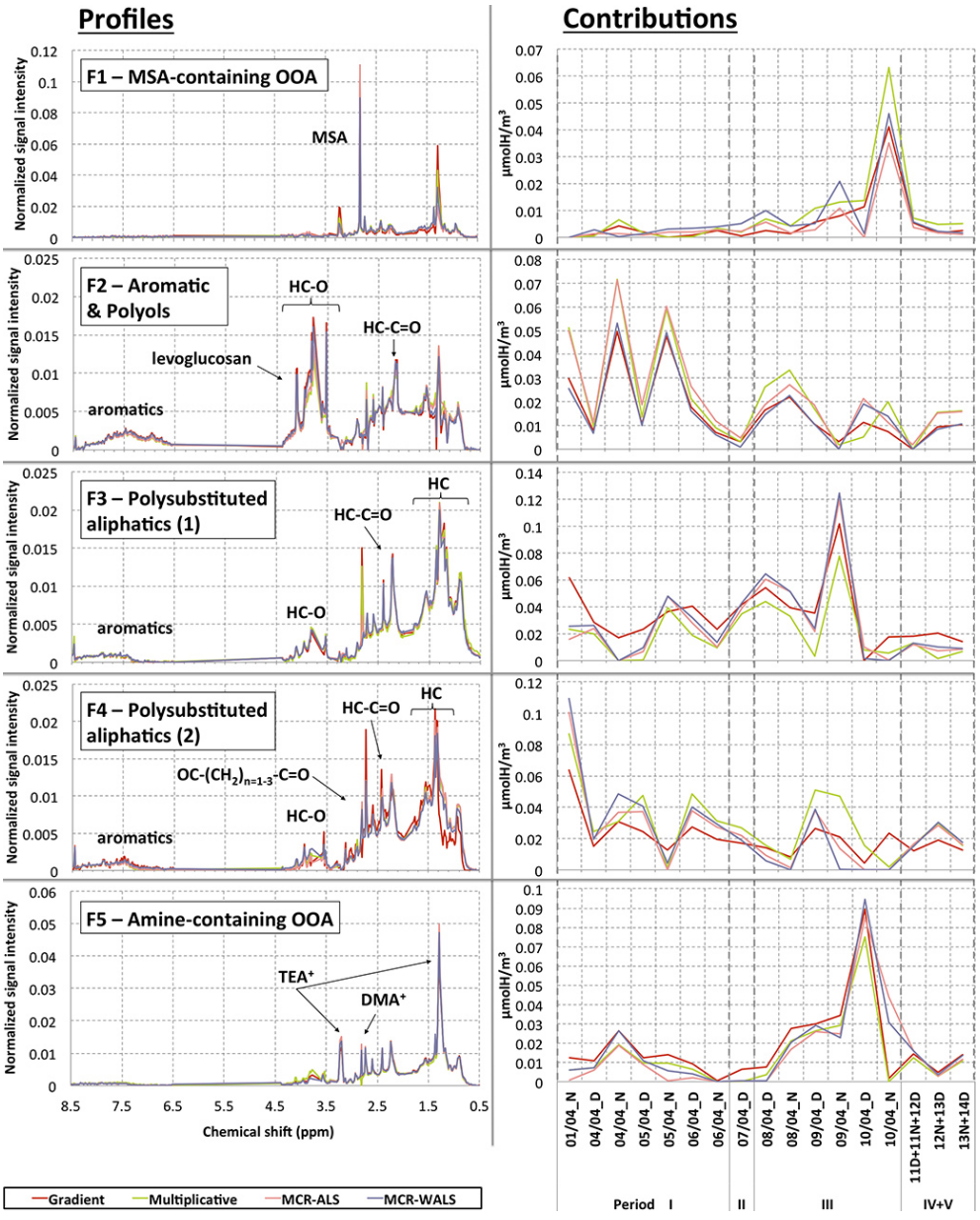

Figure 5. Profiles and contributions of five-factor solutions from ^{1}H-NMR spectra factor analysis. Results from all four different algorithms were reported: the projected gradient (red line), Multiplicative (green line), MCR-ALS (orange line) and MCR-WALS (violet line). The signal intensity of the spectral profiles was normalized (integral = 1). The samples suffixes indicate day-time (_D) and night-time (_N) sampled filters. For more details refer to the text.

Table 4. Pearson correlation coefficients (R) between NMR WSOC factors and simple chemical tracers. Only R values > 0.3 are shown.

	Cl^-	NO_3^-	SO_4^{2-}	Na^+	NH_4^+	K^+	Levoglucosan
NMR Factor 1							
NMR Factor 2					0.30	0.71	0.98
NMR Factor 3						0.33	
NMR Factor 4		0.55	0.68	0.37	0.57	0.69	
NMR Factor 5	0.58	0.45	0.45		0.50		

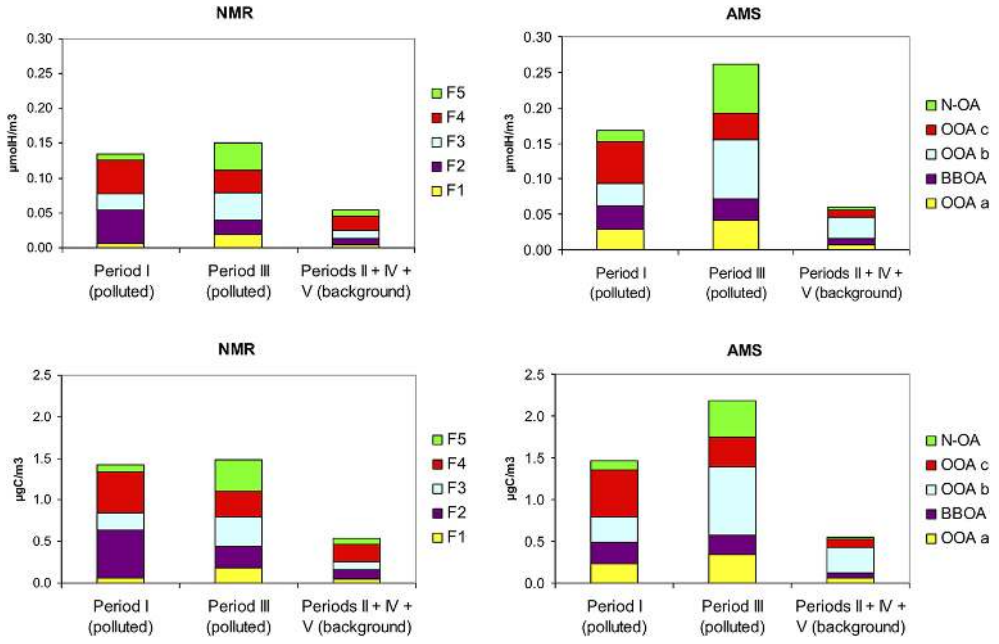

Figure 6. Average concentrations of NMR and AMS factors for WSOC and OOA, respectively, in the three main periods of the field campaign. Concentrations are expressed in hydrogen (upper panels) and carbon units (lower panels).

Table 5. Correlation matrix between NMR and AMS factors. Only R values > 0.3 are shown.

	OOAc	N–OA	OOAa	OOAb	HOA	BBOA
NMR Factor 1				0.51		
NMR Factor 2	0.74		0.57		0.85	0.79
NMR Factor 3		0.45	0.43			0.34
NMR Factor 4	0.78				0.36	0.32
NMR Factor 5		0.50		0.63		

processing of biological material remains low. In fact, factor analysis clearly splits between MSA and amines. F1 correlates positively with chloride, but this cannot be clarified fully by simple chemical tracer analysis.

– NMR Factor 2 (F2: "aromatic and polyols") is characterized by a spectral profile showing clear signatures from aromatic compounds and polyols, closely matching the spectra of biomass burning aerosols obtained in the laboratory (see Sect. 4). The good correlation of F2 contributions with the concentrations of levoglucosan and potassium ($R = 0.98$ and 0.71, respectively) supports the link between F2 and primary wood burning products. F2 concentrations showed highest levels in Period I of the campaign, with a marked diurnal variability with maxima at night-time, indicating production from ground sources and atmospheric accumulation/dispersion governed by the diurnal cycle of the planetary boundary layer during days of high-pressure conditions. Such a pattern has already been observed for NO_x and for HOA and BBOA in the same period of the campaign (Saarikoski et al., 2012).

– NMR Factor 3 and Factor 4 (F3 and F4: "polysubstituted aliphatics 1 and 2") show similar spectral profiles but different time trends. Even though they could result from one single factor split into two, the difference between F3 and F4 is considered real based on the fact that a four-factor solution does not recombine factors 3 and 4, and hinders the identification of the other factors compared to the chosen five-factor solution. Their spectral profiles are characterized by polysubstituted aliphatic moieties and some hydroxyl groups (between 3.2 and 4.5 ppm) with a smaller contribution from aromatics. The spectrum of F3 shows greater contributions from aliphatic chains (δH $\sim$ 1.3 ppm) and from hydroxyl groups with respect to F4. Aromaticity is low, indicating that the aliphatic compounds responsible for the resonances between 1.8 and 3.2 ppm are substituted mainly with carbonyls or carboxylic acids. Overall, such spectral features are compatible with the composition

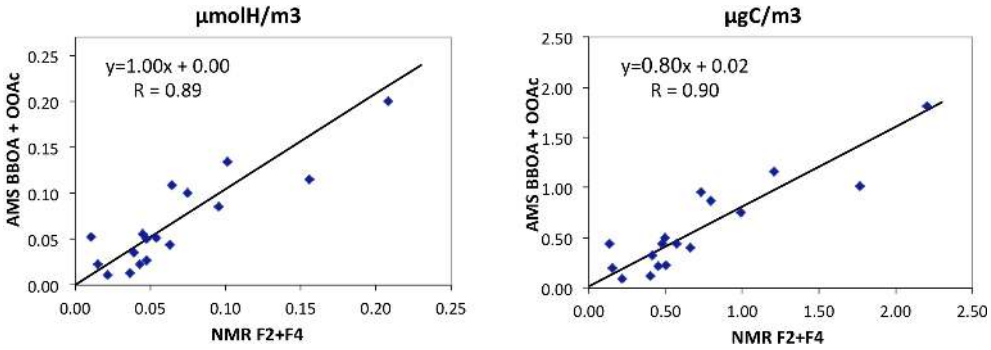

Figure 7. Correlation plots between NMR and AMS total biomass burning contributions: NMR F2 and F4, and AMS BBOA and OOAc). An orthogonal fitting was used for the regression lines.

of secondary organic aerosols (SOA). F3 concentrations are greater during (polluted) Period III of the campaign, while F4 is found in all periods, with little variability between polluted and background conditions. F3 does not correlate with any simple chemical tracer (Table 4) except potassium. F4 is correlated with secondary species (ammonium, sulfate, nitrate) and with potassium. The correlation of potassium with F4 is much stronger than with F3, and comparable to that with F2. Therefore, F4 is another candidate biomass burning factor, but, given its correlation with secondary inorganic species, much more *aged* than F2, which is consistent with its low correlation with levoglucosan and the functional group composition dominated by carboxyls and carbonyls. The interrelationship of NMR factors F2 and F4 will be discussed in more detail in Sect. 4.

– NMR Factor 5 (F5: "amines") shows the contributions from the low-molecular-weight amines introduced in Sect. 3.2. Traces of MSA and unresolved aliphatic compounds provide additional contributions to the spectrum of F5. Possible emissions from local husbandry and agricultural practices have already been mentioned. Period III of the campaign was characterized by a stably stratified atmosphere, low maximum temperatures and high humidity (Saarikoski et al., 2012), with conditions favorable for the formation of particulate nitrate, which indeed showed the highest concentrations of the campaign in those days. The correlation between F5 and aerosol nitrate suggests that the low-molecular-weight amines occurred in the aerosol mainly as aminium nitrate and that its formation was regulated by gas/particle partitioning similar to that for ammonium nitrate.

It should be noted that this analysis identified factors that represent extremes in the functional group distributions observed for the samples (Fig. 3), with F2 showing the highest hydroxyl content (lower right corner of the diagram in Fig. 3, panel a), F3 and F4 representing compounds with the highest content of aliphatic groups substituted with carbonyls and

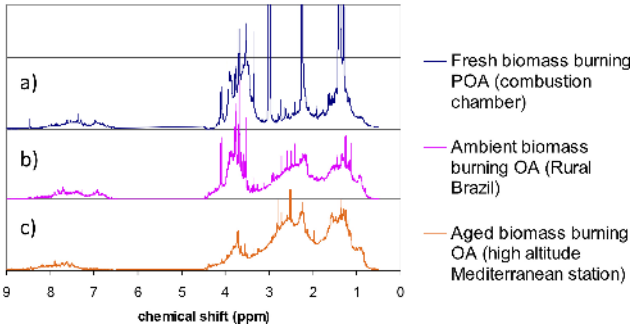

Figure 8. Reference ^{1}H-NMR spectra for different stages of biomass burning aerosol ageing: **(a)** laboratory wood burning POA (the sharp peaks at 1.3, 2.2 and 3.3 ppm are from contaminants); **(b)** ambient near-source biomass burning aerosol; **(c)** biomass burning aerosol from long-range transport.

carboxyls (upper left corner), and F1 and F5 accounting for the species enriched in heteroatoms (lower left corner).

3.5 Comparison between NMR and AMS factor analyses

The PMF–AMS factors for organic aerosol in San Pietro Capofiume (cf. Figs. 7 and 8 in Saarikoski et al., 2012) were averaged over the filter-sampling intervals aiming to compare with the NMR factors for WSOC. The correlation coefficients between the resulting AMS factor time trends and the NMR factor contributions (Fig. 5) are reported in Table 5. Average concentrations in molH m^{-3} and µgC m^{-3} for the AMS and NMR factors in the two polluted periods and for background conditions are presented in Fig. 6. The HOA contribution is excluded from this mass budget as it is not expected to contribute to WSOC. As already discussed in Sect. 3.1, there is an excess of the AMS concentrations in molH m^{-3} compared to NMR, which is not so evident when using carbon concentrations (Fig. 1). This reflects the greater H / C ratios provided by the AMS analysis with respect to the NMR method, as the latter is blind to hydrogen atoms

bound to oxygen or nitrogen atoms, which contribute to the fragments in the AMS spectra. When considering the factor budget in carbon units, the total AMS concentrations exceeds the NMR concentrations only in the second polluted period (or Period III), as already discussed in Sect. 3.1.

The correlation analysis (Table 5) suggests possible overlaps between the NMR and AMS factors. In particular, the NMR factor for fresh biomass burning (F2) shows strong positive correlations with the AMS combustion factors (BBOA and HOA), but moderate correlations were also found with OOAa, which is of secondary origin, and especially with OOAc, which is a class of oxygenated aerosols associated with biomass burning (Saarikoski et al., 2012). Positive but modest correlations were also found between the AMS primary combustion factors (BBOA and HOA) and NMR F4, which in turn shows the highest correlation with AMS OOAc. Therefore, there is clearly a link between biomass burning and AMS BBOA (primary), OOAc (oxygenated), as well as NMR factors F2 (primary) and F4 (processed). On the basis of the correlation coefficients, a tentative assignment of NMR F2 to BBOA and NMR F4 to OOAc could be postulated. The functional group composition of NMR F2 indicates a much greater oxidation state than that of BBOA. In fact, F2 recovers the anhydrosugars that were shown to correlate poorly with BBOA, while showing a clearer link with OOAc (Saarikoski et al., 2012). Therefore, the "fresh" and "processed" portions of biomass burning aerosol in NMR factorization do not overlap fully with those from PMF-AMS: while PMF-AMS split the two classes according to their oxygen content, NMR factor analysis was more sensitive to differences in functional group distribution (phenols and polyols vs. carbonyls and carboxyls).

Since the spectral variability and corresponding noise levels of features corresponding to different functionalities are not identical between AMS and NMR, it is not surprising that the PMF factors that are extracted from the two data sets are not identical. PMF solutions also generally have a rotational ambiguity that could result in the fresh and processed biomass burning factors being separated from each other to a different extent in the two different analyses. An important difference between the two methodologies is that the AMS data set accounts for species that are water insoluble (i.e., HOA) and are not included in the NMR data set. Finally, the different time resolution of AMS and NMR data could play an important role in the PMF ability to separate organic classes. Thus, AMS components often reflect not only differences in chemical composition, but also differences in volatility that are likely worse resolved on the 12 h time resolution of the NMR data. Despite the differences in the individual components extracted from the AMS and NMR, the correlation between the sum of fresh and aged biomass burning fractions in the AMS and those from NMR analysis was very good ($R = 0.89$ in terms of $\mu molH\,m^{-3}$ and 0.90 in terms of $\mu gC\,m^{-3}$, see Fig. 7). Clearly, the two techniques agreed well on the fact that two factors are needed to apportion the biomass burning sources of the organic aerosol during the 2008 EUCAARI campaign in the Po Valley.

Finally, Table 5 shows a positive correlation also between the AMS nitrogenated compounds (N-OA) and the NMR factor for amines, indicating that aliphatic amines contributed to the nitrogen content of OOA measured by the HR-TOF-AMS. The correlation is not strong, which may be explained by the fact that most low-molecular-weight amines can occur as nitrate salts, which are semivolatile, hence prone to sampling artifacts when collected using filters. Both NMR F4 and AMS N-OA occur in greater concentrations during Period III, when high relative humidities favored the partitioning of nitric acid and atmospheric volatile bases into particles.

4 Contribution of biomass burning POA and SOA

The examination of NMR and AMS factors in search of biomass burning aerosol components led to the following conclusions:

1. An agreement between the NMR and AMS source apportionment for biomass burning aerosol could be achieved only by considering suitable lumpings of factors.

2. Both NMR and AMS factor analyses suggest that biomass burning aerosols include a first component linked to surface sources in the Po Valley and active at night, plus a second component better mixed in the atmosphere and prevalent in daytime that can be tagged as "fresh" and "aged" fractions, respectively.

3. The AMS BBOA would then account only for the fresh component.

4. The split between the fresh and aged biomass burning aerosols is performed differently by NMR and AMS.

In the present section, we compare the NMR factors obtained from our analysis with biomass burning aerosols generated under laboratory conditions. At present we are able to characterize only biomass burning POA using the set-up described in Sect. 2.4. For example, the ^{1}H-NMR spectrum of biomass burning aerosols generated in a log-wood stove under controlled experimental conditions (Heringa et al., 2011) shows (Fig. 8a) evident resonances from aromatic moieties including phenols and from hydroxylated compounds including levoglucosan, plus lower proportions of other aliphatic compounds. It should be noted that levoglucosan does not account for more than 15 % of total hydroxyl groups, indicating that they occur largely as an unresolved complex mixture possibly including oligomers. Similar results were obtained in a smog chamber at the Max Planck Institute for Chemistry during the intercomparison experiment prior to the 2002 SMOCC campaign (unpublished data). These data are also consistent with the spectra reported by Kubatova et

al. (2009), and provide confirmation that freshly produced particles, i.e., POA, account for the large fraction of aromatic and hydroxylated groups typical of water-soluble biomass burning aerosol (Decesari et al., 2007; Zelenay et al., 2011). In agreement with the smog chamber data, we then conclude that NMR Factor 2, "aromatic & polyols", during the 2008 EUCAARI campaign corresponded to biomass burning POA.

The spectral features of Factor 4, which we also attribute to biomass burning sources, are less characteristic and their link to chemical speciation data obtained in smog chambers is less clear. The spectral profile suggests a mix of aromatic compounds depleted in phenols and richer in electron-withdrawing substituents (like carbonylic, carboxylic or nitro groups) mixed with a (larger) fraction of aliphatic compounds substituted with unsaturated oxygenated carbon atoms, like carbonyls or carboxyls but with only a few alcohols. Therefore, Factor 4 lacks compounds most characteristic of fresh smoke particles like anhydrosugars and phenols. Nevertheless, carboxylic acids were found in significant amounts in *ambient* biomass burning aerosols (Fig. 8b; Mayol-Bracero et al., 2002; Decesari et al., 2006). Ion-exchange chromatographic techniques have been applied to separate the polyol fraction of WSOC from the carboxylic acids, including the humic-like substances (HULIS) in ambient smoke particles, showing that the concentration of the total acids can rival that of the alcohols (Decesari et al., 2006). We have reproduced the chromatographic fractionation employed for the SMOCC biomass burning experiment in Brazil, by analyzing one EUCAARI sample (from 4 April, night-time) showing highest contributions of factors 2 and 4. The ^{1}H-NMR spectra recorded for the resulting chemical classes, namely neutral/basic compounds, mono- and di-carboxylic acids, and polyacids (HULIS), are shown in Fig. 9. As during SMOCC, the fractionation of the Po Valley sample led to a clear split of the aliphatic components of WSOC, with most of the hydroxylated species and amines recovered in the neutral/basic compounds and most of the aliphatic compounds substituted with carbonyls/carboxyls falling in the acidic classes. The separation of the aromatic groups is less clear, although the polyacids (HULIS) exhibit the highest degree of aromaticity. These results support the factor analysis, indicating that polyols and the compounds enriched with H–C–C=O groups belong to different chemical classes, which are tagged here as neutral/basic compounds and mono-/di-carboxylic acids and polyacids, respectively. The comparison between factor profiles and the spectra of the chemical classes actually separated by liquid chromatography indicates that the compounds responsible for Factor 4 and associated with biomass burning sources but *not* correlating with levoglucosan and phenols must be searched in the chemical class of mono- and di-carboxylic acids, operationally defined by the ion-exchange chromatographic method.

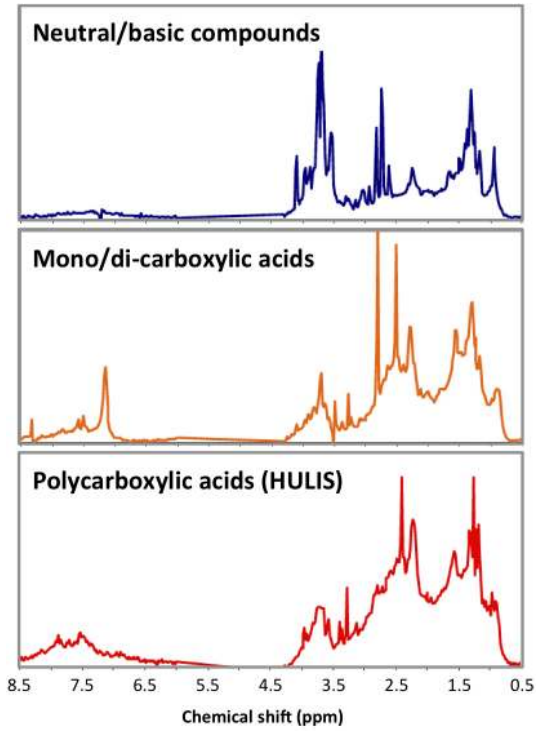

Figure 9. ^{1}H-NMR spectra of WSOC fractions isolated by anion-exchange chromatography.

During the SMOCC experiment, a greater ratio between acids with respect to polyols was found in daytime hours and was attributed to the different burning conditions in the area: more smoldering at night vs. more active flaming in the day (Decesari et al., 2006). During the first period of the EUCAARI campaign, the same was observed in an area where biomass burning is essentially due to domestic heating at night-time. An alternative explanation, more suitable for the conditions encountered during EUCAARI, is that the daytime samples, richer in carboxylic acids and depleted of polyols, are the result of atmospheric processing. Ageing would trigger the observed change in functional group distribution as a function of the O_3 / NO_2 ratio (Fig. 3) and Factor 4 would then correspond to biomass burning SOA.

To test the above hypothesis, more information about the NMR spectral characteristics of biomass burning SOA must be collected in the laboratory using smog chambers with the appropriate photochemical aging. Finding "clean" fingerprints for biomass burning SOA in ambient conditions can be challenging due to interfering source contributions. The best opportunities are large plumes from open burning in the tropics captured after several hours of transport in the middle troposphere (Capes et al., 2008). In 2007, we fortuitously captured one such event at the GAW station of Monte Cimone. Smoke particles had travelled above the planetary boundary layer for 75 to 90 h from North Africa and reached the northern coast of the Mediterranean at an altitude of about 2000 m.

For a detailed description of the event, refer to Cristofanelli et al. (2009). We discuss here the NMR characteristics of the aerosol sampled in those days, as it can be considered a good example of very aged ambient biomass burning organic aerosol. The spectrum, reported in Fig. 8c, has clearly little to do with the profile of Factor 2 and with the fingerprint of fresh smoke particles determined during the EUCAARI campaign. In fact, the composition of the Monte Cimone aged biomass burning OA lacks phenols and especially alcohols, with levoglucosan nearly absent (as partially expected also considering the instability of levoglucosan exposed to atmospheric hydroxyl radical concentrations suggested by Hennigan et al., 2010), while aliphatic compounds polysubstituted with carbonyls/carboxyls dominate. Interestingly, the spectral profile of the Monte Cimone sample shares many similarities with the polyacid (HULIS) fraction isolated from the EUCAARI sample, more than with the mono- and di-acids. These findings confirm that the compositional changes in biomass burning aerosol during long-range transport can be severe (Capes et al., 2008).

The above compilation of laboratory and ambient spectral data, although incomplete, allows one to draw the first three conclusions on the nature of NMR factors linked to biomass burning POA and SOA:

1. Data from smog chambers and from ambient samplings in near-source areas agree on showing large phenol and polyol contents in fresh particles (biomass burning POA).

2. Ambient data of very processed smoke particles show that phenols and polyols are strongly depleted and that aliphatic compounds substituted with carboxylic acids plus aromatics other than phenols account for the biomass burning SOA.

3. HULIS form and enrich with ageing in biomass burning plumes. This is consistent with the fact that the aged AMS burning related factor OOAc has a higher relative intensity of m/z 44, which is a marker of carboxylic acid formation in the AMS, compared to the fresh AMS BBOA factor.

In conclusion, specific NMR fingerprints can be derived for the fresh particles (polyols and phenols) and for the very aged biomass burning aerosol (HULIS), while less distinguishing features are available for the intermediate stage of ageing, when mono- and di-carboxylic acids are formed and the composition of biomass burning SOA overlaps with that of oxidized compounds originating from other sources, like those responsible for Factor 3 during EUCAARI. Again, this observation is consistent with AMS measurements that indicate that photochemical aging of aerosols results in increased acid content and increasingly similar AMS spectra (Cubison et al., 2011; Jolleys et al., 2012). In areas impacted by residential wood burning sources, the quality of the data set and the factor analysis will be critical for the discrimination of the NMR factor for biomass burning SOA.

Table 6. Results of ^{14}C analysis. The activities of the samples taken directly from the measurements ($F^{14}C$) are reported together with their experimental errors. The percentages of modern carbon with respect to the total were calculated taking into account two different scenarios: one in which we considered the modern carbon coming completely from biogenic aerosol (using fM(bio)=1.04) and the second one in which we considered the modern carbon derived entirely from biomass burning aerosol (using fM(bb) = 1.19).

Sample ID	$F^{14}C$	% modern $C_{(BB)}$	% modern $C_{(BIO)}$
08/04_D	0.608 ± 0.011	51 %	58 %
08/04_N	0.704 ± 0.014	59 %	68 %
09/04_D	0.542 ± 0.011	46 %	52 %
09/04_N	0.588 ± 0.014	49 %	57 %
10/04_D	0.558 ± 0.014	47 %	54 %
10/04_N	0.588 ± 0.011	49 %	57 %
11/04_D	0.534 ± 0.011	45 %	51 %
11/04_N	0.573 ± 0.011	48 %	55 %
12/04_D	0.536 ± 0.010	45 %	52 %
12/04_N	0.738 ± 0.014	62 %	71 %
13/04_D	0.609 ± 0.011	51 %	59 %
14/04_D	0.572 ± 0.011	48 %	55 %

5 Isotopic measurements and carbon budget

Modern and fossil fuel fractions of aerosol total carbon were measured in 12 samples during periods III, IV and V of the campaign (with the methods and criteria already described in Sect. 2.5) and the results are reported in Table 6. Unlike period I, where the change in aerosol composition was driven by the diurnal evolution of the boundary layer, the other periods show less clear dynamics. As a result, the small changes in modern carbon fraction between samples shown by the isotopic analysis could not be related unambiguously to any of the trends of AMS and NMR factors. Aiming to estimate the contribution of modern carbon to aerosol TC from isotopic ^{14}C measurements, assumptions about the actual reference fraction of modern carbon have to be made. As discussed previously (see Sect. 2.5), such a reference value depends on the relative influence of biomass burning sources, employing 60- to 80-old tree logs as fuel, vs. (strictly contemporary) biogenic sources. The two cases were considered here to provide a range of variation for $F^{14}C$ (Table 6). On average, $F^{14}C$ for TC was between 50 % (the biomass burning case) and 57 % (biogenic). These results are in between the values typically observed for urban sites (Yamamoto et al., 2007; Marley et al., 2009) and those representative of rural locations (Gelencser et al., 2007; Szidat et al., 2007; Hodzic et al., 2010).

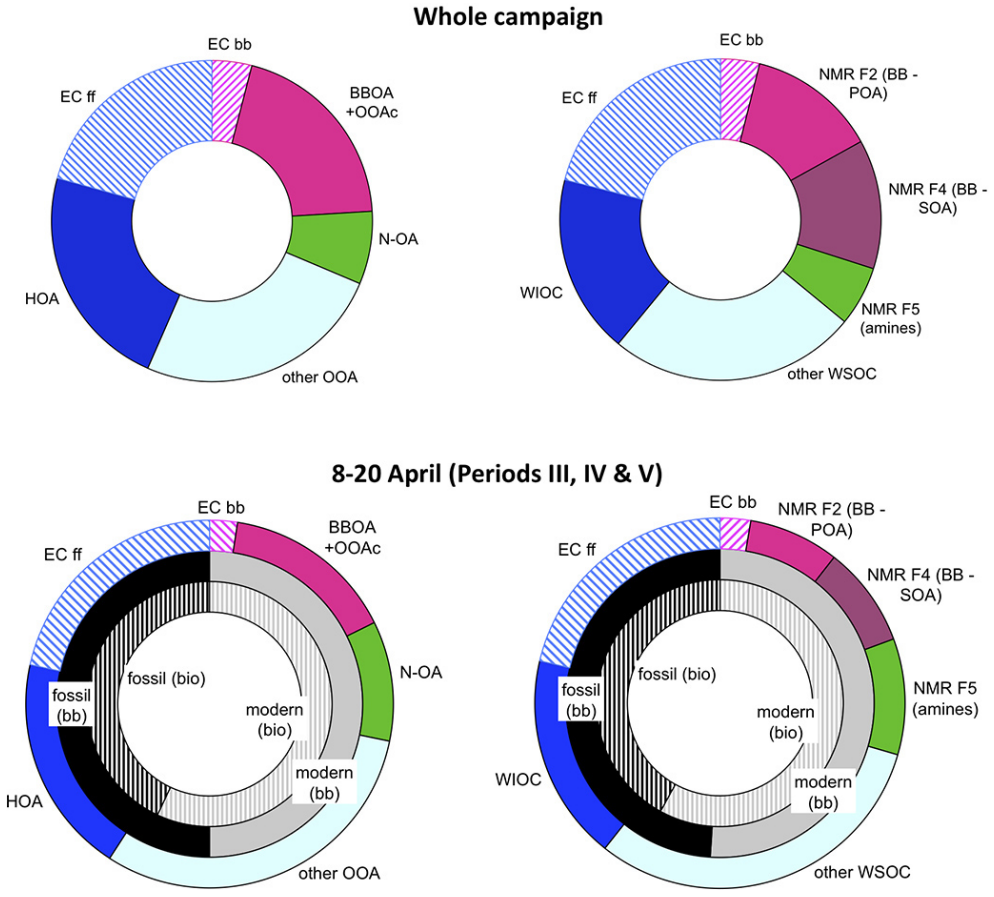

Figure 10. Carbon budget of aerosol TC for the whole campaign (upper two panels) and for the period covered by the isotopic analyses (lower panels). Budgets are reconstructed based on PMF-AMS components (left) and NMR factors for WSOC (right). For more explanations refer to the text.

Since we have already apportioned the biomass burning fraction of OC using NMR and AMS data, in this section we employ the ^{14}C data to investigate the biogenic/anthropogenic nature of the remaining oxidized organic compounds. We have calculated an aerosol carbon budget based on the following assumptions: (a) the EC / OC ratio for biomass burning aerosol was set to 0.16 based on recommendations of Szidat et al. (2006); (b) amine-containing compounds and AMS N-OA originate from emissions from livestock and other modern carbon sources; (c) primary OC from fossil fuel combustion is fully water insoluble. In addition, when comparing the carbon budget based on the AMS factors with that elaborated starting from filter analysis, we attributed AMS HOA to WIOC and BBOA and OOAc to the sum of NMR F2 and F4. The resulting calculations, as campaign averages, are reported in the upper panel of Fig. 10, and, for the days covered by isotopic analysis, in the lower panels of the same figure. It can be observed that WIOC/HOA together with the fossil fraction of EC account for most of the fossil TC: the totality of it, under the assumption of modern carbon dominated by biogenic emissions, leaving very little room for WSOC or OOA originating from fossil fuel combustion. As anticipated in the previous section, NMR and AMS fractionations agree in apportioning about one third of OC to biomass burning sources as a campaign average. As the source intensity of wood burning decreased with time (Figs. 2 and 5), the second part of the campaign, for which fossil carbon data are available, shows a lower fraction of OC apportioned to biomass burning: 20 % or 22 % based on, respectively, AMS and NMR analyses, which fall in the range indicated by the levoglucosan analyses (from 10 % to 30 %, Alves et al., 2012).

Irrespective of the hypotheses, the non-biomass burning WSOC (or OOA carbon) is predominantly accounted for by modern carbon, and therefore is of *biogenic* origin. Depending on the assumptions about the ^{14}C content of modern carbon, the fossil fraction of the non-biomass burning WSOC is only 5 to 25 %. Such biogenic nature of non-biomass burning OOA/WSOC is somewhat surprising for a polluted environment at the mid-latitudes in a period of the year (March to early April) when vegetation has just started to recover from winter dormancy. However, this result is in agreement

with known collections of ^{14}C data for atmospheric aerosols, indicating a general dominance of modern carbon sources, including polluted areas with limited evidence of biomass burning emissions (Hodzic et al., 2010).

6 Conclusions

We applied factor analysis to NMR spectroscopy for WSOC source apportionment. The 2008 EUCAARI campaign in the Po Valley was exceptional in respect to the variability in the aerosol organic composition, due to different photochemical regimes and transport conditions. NMR factor analysis identified a total of five factors. Two were associated with chemical tracers, namely MSA and low-molecular-weight amines. A third factor was clearly associated with primary wood burning particles and showed a chemical composition dominated by anhydrosugars, other polyols and phenolic compounds. The other two factors represented "aged" components, but one of the two, based on correlation with tracer compounds, was interpreted as aged biomass burning particles. Similar results are provided by PMF analysis of the AMS parallel data set. The best match between the total biomass burning fraction of OC estimated from the NMR was found when adding an oxygenated factor to the "fresh" AMS biomass burning component (BBOA). NMR factor analysis provides a differentiation between the primary oxygenated biomass burning, rich in phenols and polyols, and the secondary fraction rich in carbonylic compounds and acids (including HULIS). The overall change in composition between the "fresh" and "aged" biomass burning aerosol is also observed in the AMS biomass burning related factors.

Overall, the fraction of OC apportioned to biomass burning by PMF-AMS and NMR factor analysis varied between 20 and 29 % (i.e., 15 to 22 % of TC), in the middle–upper range of the fraction estimated by molecular marker analysis (Alves et al., 2012). Most interestingly, as the ^{14}C results indicate a modern fraction of TC of ca. 50–57 %, carbon budget calculations imply that most of the unapportioned WSOC (and OOA) is from modern carbon sources, hence biogenic. Such biogenic sources for OOA in a period of the year when terpene emissions are small cannot be explained easily based on the current knowledge about SOA formation mechanisms. One potential source of modern carbon at the site is represented by cooking aerosols (Crippa et al., 2013b; Minguillón et al., 2011; Mohr et al., 2012), which, however, were not clearly discriminated by PMF-AMS in this study. On the other hand, the occurrence of methane–sulfonate and especially of amines in large amounts in our samples suggest that the emission of reduced sulfur and nitrogen species provided an "unconventional" (non-terpene) source of biogenic SOA in the area. Notice that part of these emissions may involve anthropogenic activities, such as animal farming and waste treatment. In this sense, such biogenic sources would be still anthropogenic. Clearly, the anaerobic biotic reactions responsible for the emissions of amines occur according to completely different mechanisms with respect to the well-studied terpene emissions from living tissues of plants. Although some recent studies have examined the composition of VOCs emitted by animal farms and from their wastes, their SOA formation potential is poorly known, and, on the basis of the conclusions of our study, they deserve investigation.

The Supplement related to this article is available online at doi:10.5194/acp-14-5089-2014-supplement.

Acknowledgements. The main part of the work in this paper has been funded with FP6 project EUCAARI (contract 34684). This research, especially in respect to data analysis, was also financially supported by FP7 project PEGASOS (contract 265148).

Edited by: S. A. Nizkorodov

References

Aiken, A. C., de Foy, B., Wiedinmyer, C., DeCarlo, P. F., Ulbrich, I. M., Wehrli, M. N., Szidat, S., Prevot, A. S. H., Noda, J., Wacker, L., Volkamer, R., Fortner, E., Wang, J., Laskin, A., Shutthanandan, V., Zheng, J., Zhang, R., Paredes-Miranda, G., Arnott, W. P., Molina, L. T., Sosa, G., Querol, X., and Jimenez, J. L.: Mexico city aerosol analysis during MILAGRO using high resolution aerosol mass spectrometry at the urban supersite (T0) – Part 2: Analysis of the biomass burning contribution and the non-fossil carbon fraction, Atmos. Chem. Phys., 10, 5315–5341, doi:10.5194/acp-10-5315-2010, 2010.

Alves, C., Vicente, A., Pio, C., Kiss, G., Hoffer, A., Decesari, S., Prevot, ASH; Minguillon, MC; Querol, X., Hillamo, R., Spindler, G., and Swietlicki, E.: Organic compounds in aerosols from selected European sites – Biogenic versus anthropogenic sources, Atmos. Environ., 59, 243–255, doi:10.1016/j.atmosenv.2012.06.013, 2012.

Barmpadimos, I., Hueglin, C., Keller, J., Henne, S., and Prévôt, A. S. H.: Influence of meteorology on PM_{10} trends and variability in Switzerland from 1991 to 2008, Atmos. Chem. Phys., 11, 1813–1835, doi:10.5194/acp-11-1813-2011, 2011.

Barmpadimos, I., Keller, J., Oderbolz, D., Hueglin, C., and Prévôt, A. S. H.: One decade of parallel fine ($PM_{2.5}$) and coarse (PM_{10}–$PM_{2.5}$) particulate matter measurements in Europe: trends and variability, Atmos. Chem. Phys., 12, 3189–3203, doi:10.5194/acp-12-3189-2012, 2012.

Bond, T. C., Streets, D. G., Yarber, K. F., Nelson, S. M., Woo, J.-H., and Klimont, Z.: A Technology-based Global Inventory of Black and Organic Carbon Emissions from Combustion, J. Geophys. Res., 109, D14203, doi:10.1029/2003JD003697, 2004.

Capes, G., Johnson, B., McFiggans, G., Williams, P. I., Haywood, J., and Coe H.: Aging of biomass burning aerosols over West Africa: Aircraft measurements of chemical composition, microphysical properties, and emission ratios, J. Geophys. Res., 113, D00C15, doi:10.1029/2008JD009845, 2008.

Crippa, M., Canonaco, F., Lanz, V. A., Äijälä, M., Allan, J. D., Carbone, S., Capes, G., Dall'Osto, M., Day, D. A., DeCarlo, P. F.,

Di Marco, C. F., Ehn, M., Eriksson, A., Freney, E., Hildebrandt Ruiz, L., Hillamo, R., Jimenez, J.-L., Junninen, H., Kiendler-Scharr, A., Kortelainen, A.-M., Kulmala, M., Mensah, A. A., Mohr, C., Nemitz, E., O'Dowd, C., Ovadnevaite, J., Pandis, S. N., Petäjä, T., Poulain, L., Saarikoski, S., Sellegri, K., Swietlicki, E., Tiitta, P., Worsnop, D. R., Baltensperger, U., and Prévôt, A. S. H.: Organic aerosol components derived from 25 AMS datasets across Europe using a newly developed ME-2 based source apportionment strategy, Atmos. Chem. Phys. Discuss., 13, 23325–23371, doi:10.5194/acpd-13-23325-2013, 2013a.

Crippa, M., DeCarlo, P. F., Slowik, J. G., Mohr, C., Heringa, M. F., Chirico, R., Poulain, L., Freutel, F., Sciare, J., Cozic, J., Di Marco, C. F., Elsasser, M., Nicolas, J. B., Marchand, N., Abidi, E., Wiedensohler, A., Drewnick, F., Schneider, J., Borrmann, S., Nemitz, E., Zimmermann, R., Jaffrezo, J.-L., Prévôt, A. S. H., and Baltensperger, U.: Wintertime aerosol chemical composition and source apportionment of the organic fraction in the metropolitan area of Paris, Atmos. Chem. Phys., 13, 961–981, doi:10.5194/acp-13-961-2013, 2013b.

Cristofanelli, P., Marinoni, A., Arduini, J., Bonafè, U., Calzolari, F., Colombo, T., Decesari, S., Duchi, R., Facchini, M. C., Fierli, F., Finessi, E., Maione, M., Chiari, M., Calzolai, G., Messina, P., Orlandi, E., Roccato, F., and Bonasoni, P.: Significant variations of trace gas composition and aerosol properties at Mt. Cimone during air mass transport from North Africa – contributions from wildfire emissions and mineral dust, Atmos. Chem. Phys., 9, 4603–4619, doi:10.5194/acp-9-4603-2009, 2009.

Cubison, M. J., Ortega, A. M., Hayes, P. L., Farmer, D. K., Day, D., Lechner, M. J., Brune, W. H., Apel, E., Diskin, G. S., Fisher, J. A., Fuelberg, H. E., Hecobian, A., Knapp, D. J., Mikoviny, T., Riemer, D., Sachse, G. W., Sessions, W., Weber, R. J., Weinheimer, A. J., Wisthaler, A., and Jimenez, J. L.: Effects of aging on organic aerosol from open biomass burning smoke in aircraft and laboratory studies, Atmos. Chem. Phys., 11, 12049–12064, doi:10.5194/acp-11-12049-2011, 2011.

DeCarlo, P. F., Kimmel, J. R., Trimborn, A., Northway, M. J., Jayne, J. T., Aiken, A. C., Gonin, M., Fuhrer, K., Horvath, T., Docherty, K. S., Worsnop, D. R., and Jimenez, J. L.: Field-deployable, highresolution, time-of-flight aerosol mass spectrometer, Anal. Chem. 78, 8281–8289, 2006.

Decesari, S., Facchini, M. C., Fuzzi S., and Tagliavini, E.: Characterization of water-soluble organic compounds in atmospheric aerosol: A new approach, J. Geophys. Res., 105, 1481–1489, 2000.

Decesari, S., Facchini, M. C., Matta, E., Lettini, F., Mircea, M., Fuzzi, S., Tagliavini, E., and Putaud, J. P.: Chemical features and seasonal variation of fine aerosol water-soluble organic compounds in the Po Valley, Italy, Atmos. Environ., 35, 3691–3699, 2001.

Decesari, S., Fuzzi, S., Facchini, M. C., Mircea, M., Emblico, L., Cavalli, F., Maenhaut, W., Chi, X., Schkolnik, G., Falkovich, A., Rudich, Y., Claeys, M., Pashynska, V., Vas, G., Kourtchev, I., Vermeylen, R., Hoffer, A., Andreae, M. O., Tagliavini, E., Moretti, F., and Artaxo, P.: Characterization of the organic composition of aerosols from Rondônia, Brazil, during the LBA-SMOCC 2002 experiment and its representation through model compounds, Atmos. Chem. Phys., 6, 375–402, doi:10.5194/acp-6-375-2006, 2006.

Decesari, S., Mircea, M., Cavalli, F., Fuzzi, S., Moretti, F., Tagliavini, E. and Facchini, M. C.: Source attribution of water-soluble organic aerosol by nuclear magnetic resonance spectroscopy, Environ. Sci. Technol., 41, 2479–2484, 2007.

Decesari, S., Finessi, E., Rinaldi, M., Paglione, M., Fuzzi, S., Stephanou, E. G., Tziaras, T., Spyros, A., Ceburnis, D., O'Dowd, C., Dall'Osto, M., Harrison, R. M., Allan, J., Coe, H., and Facchini, M. C.: Primary and secondary marine organic aerosols over the North Atlantic Ocean during the MAP experiment, J. Geophys. Res., 116, D22210, doi:10.1029/2011JD016204, 2011.

Duplissy, J., DeCarlo, P. F., Dommen, J., Alfarra, M. R., Metzger, A., Barmpadimos, I., Prevot, A. S. H., Weingartner, E., Tritscher, T., Gysel, M., Aiken, A. C., Jimenez, J. L., Canagaratna, M. R., Worsnop, D. R., Collins, D. R., Tomlinson, J., and Baltensperger, U.: Relating hygroscopicity and composition of organic aerosol particulate matter, Atmos. Chem. Phys., 11, 1155–1165, doi:10.5194/acp-11-1155-2011, 2011.

Elsasser, M., Crippa, M., Orasche, J., DeCarlo, P. F., Oster, M., Pitz, M., Cyrys, J., Gustafson, T. L., Pettersson, J. B. C., Schnelle-Kreis, J., Prévôt, A. S. H., and Zimmermann, R.: Organic molecular markers and signature from wood combustion particles in winter ambient aerosols: aerosol mass spectrometer (AMS) and high time-resolved GC-MS measurements in Augsburg, Germany, Atmos. Chem. Phys., 12, 6113–6128, doi:10.5194/acp-12-6113-2012, 2012.

Freutel, F., Schneider, J., Drewnick, F., von der Weiden-Reinmüller, S.-L., Crippa, M., Prévôt, A. S. H., Baltensperger, U., Poulain, L., Wiedensohler, A., Sciare, J., Sarda-Estève, R., Burkhart, J. F., Eckhardt, S., Stohl, A., Gros, V., Colomb, A., Michoud, V., Doussin, J. F., Borbon, A., Haeffelin, M., Morille, Y., Beekmann, M., and Borrmann, S.: Aerosol particle measurements at three stationary sites in the megacity of Paris during summer 2009: meteorology and air mass origin dominate aerosol particle composition and size distribution, Atmos. Chem. Phys., 13, 933–959, doi:10.5194/acp-13-933-2013, 2013.

Ge, X., Wexler, A. S., and Clegg, S. L.: Atmospheric amines-Part 1. A review, Atmos. Environ., 45, 524–546, 2011.

Gelencsér A., Mészáros, T., Blazsó, M., Kiss, Gy., Krivácsy, Z., Molnár, A., and Mészáros, E.: Structural Characterisation of Organic Matter in Fine Tropospheric Aerosol by Pyrolysis-Gas Chromatography-Mass Spectrometry, J. Atmos. Chem., 37, 173–183, doi:10.1023/A:1006402731340, 2000.

Gelencsér, A., May, B., Simpson, D., Sánchez-Ochoa, A., Kasper-Giebl, A., Puxbaum, H., Caseiro, A., Casimiro, P., and Legrand, M.: Source apportionment of $PM_{2.5}$ organic aerosol over Europe: Primary/secondary, natural/anthropogenic, and fossil/biogenic origin, J. Geophys. Res.,: Atmos., 112, 1984–2012, doi:10.1029/2006JD008094, 2007.

Genberg, J., Stenström, K., Elfman, M., and Olsson, M.: Development of graphitization of μg-sized samples at Lund University, Radiocarbon, 52, 1270–1276, 2010.

Genberg, J., Hyder, M., Stenström, K., Bergström, R., Fors, E., Jönsson, J. Å., and Swietlicki, E.: Source apportionment of carbonaceous aerosol in Southern Sweden, Atmos. Chem. Phys., 11, 11387–11400, doi:10.5194/acp-11-11387-2011, 2011.

Gilardoni, S., Vignati, E., Cavalli, F., Putaud, J. P., Larsen, B. R., Karl, M., Stenström, K., Genberg, J., Henne, S., and Dentener, F.: Better constraints on sources of carbonaceous aerosols using a combined ^{14}C – macro tracer analysis in a European

rural background site, Atmos. Chem. Phys., 11, 5685–5700, doi:10.5194/acp-11-5685-2011, 2011.

Hallquist, M., Wenger, J. C., Baltensperger, U., Rudich, Y., Simpson, D., Claeys, M., Dommen, J., Donahue, N. M., George, C., Goldstein, A. H., Hamilton, J. F., Herrmann, H., Hoffmann, T., Iinuma, Y., Jang, M., Jenkin, M. E., Jimenez, J. L., Kiendler-Scharr, A., Maenhaut, W., McFiggans, G., Mentel, Th. F., Monod, A., Prévôt, A. S. H., Seinfeld, J. H., Surratt, J. D., Szmigielski, R., and Wildt, J.: The formation, properties and impact of secondary organic aerosol: current and emerging issues, Atmos. Chem. Phys., 9, 5155–5236, doi:10.5194/acp-9-5155-2009, 2009.

Hand, J. L., Schichtel, B. A., Malm, W. C., and Pitchford, M. L.: Particulate sulfate ion concentration and SO_2 emission trends in the United States from the early 1990s through 2010, Atmos. Chem. Phys., 12, 10353–10365, doi:10.5194/acp-12-10353-2012, 2012.

Hennigan, C. J., Sullivan, A. P., Collett Jr., J. L., and Robinson, A. L.: Levoglucosan stability in biomass burning particles exposed to hydroxyl radicals, Geophys. Res. Lett., 37, L09806, doi:10.1029/2010GL043088, 2010.

Harrison, R. M. and Yin, J.: Sources and processes affecting carbonaceous aerosol in central England, Atmos. Environ., 42-7, 1413–1423, doi:10.1016/j.atmosenv.2007.11.004, 2008.

Heringa, M. F., DeCarlo, P. F., Chirico, R., Tritscher, T., Dommen, J., Weingartner, E., Richter, R., Wehrle, G., Prévôt, A. S. H., and Baltensperger, U.: Investigations of primary and secondary particulate matter of different wood combustion appliances with a high-resolution time-of-flight aerosol mass spectrometer, Atmos. Chem. Phys., 11, 5945–5957, doi:10.5194/acp-11-5945-2011, 2011.

Heringa, M. F., DeCarlo, P. F., Chirico, R., Tritscher, T., Clairotte, M., Mohr, C., Crippa, M., Slowik, J. G., Pfaffenberger, L., Dommen, J., Weingartner, E., Prévôt, A. S. H., and Baltensperger, U.: A new method to discriminate secondary organic aerosols from different sources using high-resolution aerosol mass spectra, Atmos. Chem. Phys., 12, 2189–2203, doi:10.5194/acp-12-2189-2012, 2012.

Hodzic, A., Jimenez, J. L., Prévôt, A. S. H., Szidat, S., Fast, J. D., and Madronich, S.: Can 3-D models explain the observed fractions of fossil and non-fossil carbon in and near Mexico City?, Atmos. Chem. Phys., 10, 10997–11016, doi:10.5194/acp-10-10997-2010, 2010..

Jaumot, J., Gargallo, R., de Juan, A., Tauler, R.: A graphical user-friendly interface for MCR-ALS: a new tool for multivariate curve resolution in MATLAB, Chemometrics And Intelligent Laboratory Systems, 76, 101–110, May 2005.

Jolleys, M. D., Coe, H., McFiggans, G., Capes, G., Allan, J. D., Crosier, J., Williams, P. I., Allen, G., Bower, K. N., Jimenez, J. L., Russell, L. M., Grutter, M., and Baumgardner, D.: Characterizing the Aging of Biomass Burning Organic Aerosol by Use of Mixing Ratios: A Meta-analysis of Four Regions, Environ. Sci. Technol., 46, 13093–13102, 2012.

Karakach, T., K., Knight, R., Lenz, E. M., Viant, M. R., and Walter, J. A.: Analysis of time course ^{1}H NMR metabolomics data by multivariate curve resolution, Magn. Reson. Chem., 47, Suppl 1, S105–117, 2009.

Kiendler-Scharr, A., Zhang, Q., Hohaus, T., Kleist, E., Mensah, A., Mentel, T., Spindler, C., Uerlings, R., Tillmann, R. and Wildt, J.: Aerosol Mass Spectrometric Features of Biogenic SOA: Observations from a Plant Chamber and in Rural Atmos. Environ.s, Environ. Sci. Technol. 43, 8166–8172, 2009.

Kim, K. H.: Emissions of reduced sulfur compounds (RSC) as a landfill gas (LFG): a comparative study of young and old landfill facilities, Atmos. Environ. 40, 6567–6578, 2006.

Kondo, Y., Miyazaki, Y., Takegawa, N., Miyakawa, T., Weber, R. J., Jimenez, J. L., Zhang, Q., and Worsnop, D. R.: Oxygenated and water-soluble organic aerosols in Tokyo, J. Geophys. Res.,, 112, D011203, doi:10.1029/2006JD007056, 2007.

Kubátová, A., Lahren, T. J., Beránek, J., Smoliakova, I. P., Braun, A., and Huggins, F. E.: Extractable Organic Carbon and its Differentiation by Polarity in Diesel Exhaust, Wood Smoke, and Urban Particulate Matter, Aerosol Sci. Technol., 43, 714–729, doi:10.1080/02786820902889853, 2009.

Kulmala, M., Asmi, A., Lappalainen, H. K., Baltensperger, U., Brenguier, J.-L., Facchini, M. C., Hansson, H.-C., Hov, Ø., O'Dowd, C. D., Pöschl, U., Wiedensohler, A., Boers, R., Boucher, O., de Leeuw, G., Denier van der Gon, H. A. C., Feichter, J., Krejci, R., Laj, P., Lihavainen, H., Lohmann, U., McFiggans, G., Mentel, T., Pilinis, C., Riipinen, I., Schulz, M., Stohl, A., Swietlicki, E., Vignati, E., Alves, C., Amann, M., Ammann, M., Arabas, S., Artaxo, P., Baars, H., Beddows, D. C. S., Bergström, R., Beukes, J. P., Bilde, M., Burkhart, J. F., Canonaco, F., Clegg, S. L., Coe, H., Crumeyrolle, S., D'Anna, B., Decesari, S., Gilardoni, S., Fischer, M., Fjaeraa, A. M., Fountoukis, C., George, C., Gomes, L., Halloran, P., Hamburger, T., Harrison, R. M., Herrmann, H., Hoffmann, T., Hoose, C., Hu, M., Hyvärinen, A., Hõrrak, U., Iinuma, Y., Iversen, T., Josipovic, M., Kanakidou, M., Kiendler-Scharr, A., Kirkevåg, A., Kiss, G., Klimont, Z., Kolmonen, P., Komppula, M., Kristjánsson, J.-E., Laakso, L., Laaksonen, A., Labonnote, L., Lanz, V. A., Lehtinen, K. E. J., Rizzo, L. V., Makkonen, R., Manninen, H. E., McMeeking, G., Merikanto, J., Minikin, A., Mirme, S., Morgan, W. T., Nemitz, E., O'Donnell, D., Panwar, T. S., Pawlowska, H., Petzold, A., Pienaar, J. J., Pio, C., Plass-Duelmer, C., Prévôt, A. S. H., Pryor, S., Reddington, C. L., Roberts, G., Rosenfeld, D., Schwarz, J., Seland, Ø., Sellegri, K., Shen, X. J., Shiraiwa, M., Siebert, H., Sierau, B., Simpson, D., Sun, J. Y., Topping, D., Tunved, P., Vaattovaara, P., Vakkari, V., Veefkind, J. P., Visschedijk, A., Vuollekoski, H., Vuolo, R., Wehner, B., Wildt, J., Woodward, S., Worsnop, D. R., van Zadelhoff, G.-J., Zardini, A. A., Zhang, K., van Zyl, P. G., Kerminen, V.-M., S Carslaw, K., and Pandis, S. N.: General overview: European Integrated project on Aerosol Cloud Climate and Air Quality interactions (EUCAARI) – integrating aerosol research from nano to global scales, Atmos. Chem. Phys., 11, 13061–13143, doi:10.5194/acp-11-13061-2011, 2011.

Lanz, V. A., Alfarra, M. R., Baltensperger, U., Buchmann, B., Hueglin, C., and Prévôt, A. S. H.: Source apportionment of submicron organic aerosols at an urban site by factor analytical modelling of aerosol mass spectra, Atmos. Chem. Phys., 7, 1503–1522, doi:10.5194/acp-7-1503-2007, 2007.

Lee, D. and Seung, H.: Algorithms for non-negative matrix factorization, Adv. Neural Inform. Process. Syst., 13, 556–562, 2001.

Lin, C.-J.: Projected Gradient methods for Non-negative matrix factorization, Neural Comput., 19, 2756–2779, 2007.

Mancinelli, V., Rinaldi, M., Finessi, E., Emblico, L., Mircea, M., Fuzzi, S., Facchini, M. C., andDecesari, S.: An anion-exchange

high-performance liquid chromatography method coupled to total organic carbon determination for the analysis of water-soluble organic aerosols, J. Chromatogr. A., 18, 1149, 385–389, 2007.

Manninen, H. E., Nieminen, T., Asmi, E., Gagné, S., Häkkinen, S., Lehtipalo, K., Aalto, P., Vana, M., Mirme, A., Mirme, S., Hõrrak, U., Plass-Dülmer, C., Stange, G., Kiss, G., Hoffer, A., Törő, N., Moerman, M., Henzing, B., de Leeuw, G., Brinkenberg, M., Kouvarakis, G. N., Bougiatioti, A., Mihalopoulos, N., O'Dowd, C., Ceburnis, D., Arneth, A., Svenningsson, B., Swietlicki, E., Tarozzi, L., Decesari, S., Facchini, M. C., Birmili, W., Sonntag, A., Wiedensohler, A., Boulon, J., Sellegri, K., Laj, P., Gysel, M., Bukowiecki, N., Weingartner, E., Wehrle, G., Laaksonen, A., Hamed, A., Joutsensaari, J., Petäjä, T., Kerminen, V.-M., and Kulmala, M.: EUCAARI ion spectrometer measurements at 12 European sites – analysis of new particle formation events, Atmos. Chem. Phys., 10, 7907–7927, doi:10.5194/acp-10-7907-2010, 2010.

Marley, N. A., Gaffney, J. S., Tackett, M., Sturchio, N. C., Heraty, L., Martinez, N., Hardy, K. D., Marchany-Rivera, A., Guilderson, T., MacMillan, A., and Steelman, K.: The impact of biogenic carbon sources on aerosol absorption in Mexico City, Atmos. Chem. Phys., 9, 1537–1549, doi:10.5194/acp-9-1537-2009, 2009.

Mayol-Bracero, O. L., Guyon, P., Graham, B., Roberts, G., Andreae, M. O., Decesari, S., Facchini, M. C., Fuzzi, S., and Artaxo, P.: Water-soluble organic compounds in biomass burning aerosols over Amazonia 2. Apportionment of the chemical composition and importance of the polyacidic fraction, J. Geophys. Res., 107, 8091, doi:10.1029/2001JD000522, 2002.

Minguillón, M. C., Perron, N., Querol, X., Szidat, S., Fahrni, S. M., Alastuey, A., Jimenez, J. L., Mohr, C., Ortega, A. M., Day, D. A., Lanz, V. A., Wacker, L., Reche, C., Cusack, M., Amato, F., Kiss, G., Hoffer, A., Decesari, S., Moretti, F., Hillamo, R., Teinilä, K., Seco, R., Peñuelas, J., Metzger, A., Schallhart, S., Müller, M., Hansel, A., Burkhart, J. F., Baltensperger, U., and Prévôt, A. S. H.: Fossil versus contemporary sources of fine elemental and organic carbonaceous particulate matter during the DAURE campaign in Northeast Spain, Atmos. Chem. Phys., 11, 12067–12084, doi:10.5194/acp-11-12067-2011, 2011.

Mohr, C., DeCarlo, P. F., Heringa, M. F., Chirico, R., Slowik, J. G., Richter, R., Reche, C., Alastuey, A., Querol, X., Seco, R., Peñuelas, J., Jiménez, J. L., Crippa, M., Zimmermann, R., Baltensperger, U., and Prévôt, A. S. H.: Identification and quantification of organic aerosol from cooking and other sources in Barcelona using aerosol mass spectrometer data, Atmos. Chem. Phys., 12, 1649–1665, doi:10.5194/acp-12-1649-2012, 2012.

Moretti, F., Tagliavini, E., Decesari, S., Facchini, M. C., Rinaldi, M., and Fuzzi, S.: NMR determination of total carbonyls and carboxyls: a tool for tracing the evolution of atmospheric oxidized organic aerosols, Environ. Sci. Technol., 42, 4844–4849, 2008.

Nordin, E. Z., Eriksson, A. C., Roldin, P., Nilsson, P. T., Carlsson, J. E., Kajos, M. K., Hellén, H., Wittbom, C., Rissler, J., Löndahl, J., Swietlicki, E., Svenningsson, B., Bohgard, M., Kulmala, M., Hallquist, M., and Pagels, J. H.: Secondary organic aerosol formation from idling gasoline passenger vehicle emissions investigated in a smog chamber, Atmos. Chem. Phys., 13, 6101–6116, doi:10.5194/acp-13-6101-2013, 2013.

Reimer, P. J., Brown, T. A., and Reimer, R. W.: Discussion: reporting and calibration of post-bomb ^{14}C data, Radiocarbon, 46, 1299–1304, 2004.

Rinaldi, M., Emblico, L., Decesari, S., Fuzzi, S., Facchini, M. C., and Librando, V.: Chemical characterization and source apportionment of size-segregated aerosol collected at an urban site in Sicily, Water Air Soil Pollut., 185, 311–321, doi:10.1007/s11270-007-9455-4, 2007.

Robinson, A. L., Donahue, N. M., Shrivastava, M. K., Weitkamp, E. A., A. M. Sage, Grieshop, A. P., Lane, T. E., Pierce, J. R., and Pandis, S. N.: Rethinking organic aerosols: Semivolatile emissions and photochemical aging, Science, 315, 1259–1262, 2007.

Saarikoski, S., Carbone, S., Decesari, S., Giulianelli, L., Angelini, F., Canagaratna, M., Ng, N. L., Trimborn, A., Facchini, M. C., Fuzzi, S., Hillamo, R., and Worsnop, D.: Chemical characterization of springtime submicrometer aerosol in Po Valley, Italy, Atmos. Chem. Phys., 12, 8401–8421, doi:10.5194/acp-12-8401-2012, 2012.

Skog, G.: The single stage AMS machine at Lund University: Status report, Nucl. Instr. Meth. B, 259, 1–6, 2007.

Skog, G., Rundgren, M., and Sköld, P.: Status of the Single Stage AMS machine at Lund University after 4 years of operation, Nucl. Instr. Meth. B, 268, 895–897, 2010.

Szidat, S., Jenk, T. M., Synal, H.-A., Kalberer, M., Wacker, L., Hajdas, I., Kasper-Giebl, A., and Baltensperger, U.: Contributions of fossil fuel, biomass burning, and biogenic emissions to carbonaceous aerosols in Zurich as traced by ^{14}C, J. Geophys. Res., 111, D07206, doi:10.1029/2005JD006590, 2006.

Szidat, S., Prévôt, A. S. H., Sandradewi, J., Alfarra, M. R., Synal, H.- A., Wacker, L., and Baltensperger, U.: Dominant impact of residential wood burning on particulate matter in Alpine valleys during winter, Geophys. Res. Lett., 34, L05820, doi:10.1029/2006GL028325, 2007.

Tagliavini, E., Moretti, F., Decesari, S., Facchini, M. C., Fuzzi, S., and Maenhaut, W.: Functional group analysis by H NMR/chemical derivatization for the characterization of organic aerosol from the SMOCC field campaign, Atmos. Chem. Phys., 6, 1003–1019, doi:10.5194/acp-6-1003-2006, 2006.

Tauler R.: Multivariate Curve Resolution applied to second order data, Chem. Int. Laborat. Syst., 30, 133–146, 1995.

Terrado, M., Barcelo, D., and Tauler, R.: Multivariate curve resolution of organic pollution patterns in the Ebro River surface water-groundwater-sediment-soil system, Anal. Chim. Acta, 657, 19–27, doi:10.1016/j.aca.2009.10.026, 2010.

Viana, M., Kuhlbusch, T. A. J., Querol, X., Alastuey, A., Harrison, R. M., Hopke, P. K., Winiwarter, W., Vallius, M., Szidat, S., Prévôt, A. S. H., Hueglin, C., Bloemen, H., Wåhlin, P., Vecchi, R., Miranda, A. I., Kasper-Giebl, A., Maenhaut, W., and Hitzenberger, R.: Source apportionment of particulate matter in Europe: a review of methods and results, J. Aerosol Sci., 39, 827–849, 2008.

Wentzell, P. D., Karakach, T. K., Roy, S., Martinez, M. J., Allen, C. P., Werner-Washburne, M.: Multivariate curve resolution of time course microarray data, BMC Bioinformatics, 7, 343–362, 2006.

Yamamoto, N., Muramoto, A., Yoshinaga, J., Shibata, K., Endo, M., Endo, O., Hirabayashi, M., Tanabe, K., Goto, S., Yoneda, M., and Shibata, Y.: Comparison of carbonaceous aerosols in Tokyo before and after implementation of diesel exhaust restrictions, Environ. Sci. Technol., 15, 6357–6362, 2007.

Zelenay, V., Mooser, R., Tritscher, T., Křepelová, A., Heringa, M. F., Chirico, R., Prévôt, A. S. H., Weingartner, E., Baltensperger, U., Dommen, J., Watts, B., Raabe, J., Huthwelker, T., and Ammann, M.: Aging induced changes on NEXAFS fingerprints in individual combustion particles, Atmos. Chem. Phys., 11, 11777–11791, doi:10.5194/acp-11-11777-2011, 2011.

Zhang, Q., Worsnop, D. R., Canagaratna, M. R., and Jimenez, J. L.: Hydrocarbon-like and oxygenated organic aerosols in Pittsburgh: insights into sources and processes of organic aerosols, Atmos. Chem. Phys., 5, 3289–3311, doi:10.5194/acp-5-3289-2005, 2005.